

# A novel IL-17 signaling pathway controlling keratinocyte proliferation and tumorigenesis via the TRAF4–ERK5 axis

Ling Wu,<sup>1,6\*</sup> Xing Chen,<sup>1\*</sup> Junjie Zhao,<sup>1,7</sup> Bradley Martin,<sup>1,6</sup> Jarod A. Zepp,<sup>1,7</sup> Jennifer S. Ko,<sup>2</sup> Chunfang Gu,<sup>1</sup> Gang Cai,<sup>8</sup> Wenjun Ouyang,<sup>11</sup> Ganes Sen,<sup>1</sup> George R. Stark,<sup>3</sup> Bing Su,<sup>9,10,12,13</sup> Charlotte M. Vines,<sup>14</sup> Cathy Tournier,<sup>15</sup> Thomas A. Hamilton,<sup>1</sup> Allison Vidimos,<sup>4</sup> Brian Gastman,<sup>1,4,5</sup> Caini Liu,<sup>1</sup> and Xiaoxia Li<sup>1</sup>

<sup>1</sup>Department of Immunology, <sup>2</sup>Department of Anatomical Pathology and Clinical Pathology, <sup>3</sup>Department of Cancer Biology, <sup>4</sup>Department of Dermatology, and <sup>5</sup>Department of Plastic Surgery, Cleveland Clinic, Cleveland, OH 44195

<sup>6</sup>Department of Pathology and <sup>7</sup>Department of Molecular Medicine, Cleveland Clinic Lerner College of Medicine, Case Western Reserve University School of Medicine, Cleveland, OH 44106

<sup>8</sup>Department of Laboratory Medicine, Ruijin Hospital, <sup>9</sup>Shanghai Institute of Immunology, and <sup>10</sup>Department of Immunobiology and Microbiology, Shanghai Jiao Tong University School of Medicine, Shanghai 200025, China

<sup>11</sup>Department of Immunology, Genentech, South San Francisco, CA 94080

<sup>12</sup>Department of Immunobiology and <sup>13</sup>Vascular Biology and Therapeutics Program, Yale University School of Medicine, New Haven, CT 06520

<sup>14</sup>University of Texas at El Paso, El Paso, TX 79968

<sup>15</sup>University of Manchester, Manchester M13 9PL, England, UK

**Although IL-17 is emerging as an important cytokine in cancer promotion and progression, the underlining molecular mechanism remains unclear. Previous studies suggest that IL-17 (IL-17A) sustains a chronic inflammatory microenvironment that favors tumor formation. Here we report a novel IL-17-mediated cascade via the IL-17R–Act1–TRAF4–MEKK3–ERK5 positive circuit that directly stimulates keratinocyte proliferation and tumor formation. Although this axis dictates the expression of target genes *Steap4* (a metalloredutase for cell metabolism and proliferation) and *p63* (a transcription factor for epidermal stem cell proliferation), *Steap4* is required for the IL-17-induced sustained expansion of *p63*<sup>+</sup> basal cells in the epidermis. *P63* (a positive transcription factor for the *Traf4* promoter) induces TRAF4 expression in keratinocytes. Thus, IL-17-induced *Steap4*–*p63* expression forms a positive feedback loop through *p63*-mediated TRAF4 expression, driving IL-17-dependent sustained activation of the TRAF4–ERK5 axis for keratinocyte proliferation and tumor formation.**

## CORRESPONDENCE

Xiaoxia Li:

lix@ccf.org

OR

Caini Liu:

liuc@ccf.org

Abbreviations used: DMBA, 7,12-dimethylbenz[*a*]anthracene; ERK, extracellular signal-regulated kinase; FFPE, formalin-fixed paraffin-embedded; K5<sup>Cre</sup>, Keratin 5–Cre; NOX, NADPH oxidase; SCC, squamous cell carcinoma; TPA, 12-*O*-tetradecanoylphorbol-13-acetate; TRAF, TNF receptor-associated factor.

IL-17 (IL-17A), a signature cytokine produced by a subset of T helper cells termed Th17 cells, plays essential roles in host defense against bacterial and fungal infections (Iwakura et al., 2008; Puel et al., 2011). Chronic overproduction of IL-17 contributes to inflammatory conditions like psoriasis, multiple sclerosis, rheumatoid arthritis, and inflammatory bowel disease (Golden et al., 2013). It has long been appreciated that chronic inflammation poses a potential risk for the development of cancer. For example, patients with inflammatory bowel diseases are at high risk for developing colorectal cancer, and chronic hepatitis infections can lead to hepatocellular

carcinoma (Coussens and Werb, 2002). Inflammation and damage from long-term cigarette smoking is the major risk factor for developing lung cancer.

IL-23, an upstream cytokine of Th17 cells, is well documented in promoting tumor development by inducing and maintaining an inflammatory microenvironment optimal for tumor progression (Langowski et al., 2006; Grivennikov et al., 2012). IL-17 has more recently been detected in cancer patients and correlates with

© 2015 Wu et al. This article is distributed under the terms of an Attribution–Noncommercial–Share Alike–No Mirror Sites license for the first six months after the publication date (see <http://www.rupress.org/terms>). After six months it is available under a Creative Commons License (Attribution–Noncommercial–Share Alike 3.0 Unported license, as described at <http://creativecommons.org/licenses/by-nc-sa/3.0/>).

\*L. Wu and X. Chen contributed equally to this paper.

prognosis. High IL-17 levels in hepatocellular carcinoma, colorectal cancer, and nonsmall cell lung cancer are indicative of poorer prognosis (Zhang et al., 2009; Wilke et al., 2011). IL-17 has been shown to promote angiogenesis by up-regulating a variety of proangiogenic factors in tumor cells and fibroblasts (Numasaki et al., 2003; Liu et al., 2011). In fact, IL-17 can promote tumor resistance to anti-VEGF therapy by providing an alternative pathway for angiogenesis independent of VEGF (Chung et al., 2013). In murine models of cutaneous squamous cell carcinoma (SCC), IL-17-mediated inflammation has been shown to promote tumor formation and progression through the induction of IL-6, which in turn activates STAT3 (Wang et al., 2010; He et al., 2012). These studies so far had attributed the proinflammatory role of IL-17 to tumorigenesis (Chae et al., 2010; Hyun et al., 2012; Tong et al., 2012). However, the detailed molecular and cellular mechanism for how IL-17 promotes tumorigenesis is not completely understood.

The receptor for IL-17 (IL-17A) is a heterodimeric complex composed of two subunits, IL-17RA and IL-17RC (Toy et al., 2006; Gaffen, 2009; Zhang et al., 2014). Upon receptor binding to IL-17, the adaptor E3-ubiquitin ligase, Act1 (also known as CIKS), is recruited to mediate downstream signaling events (Chang et al., 2006; Qian et al., 2007). We as well as others have shown that TNF receptor-associated factor (TRAF) proteins are immediate binding partners of Act1 and are required for downstream pathway activation (Hartupree et al., 2009; Bulek et al., 2011; Sun et al., 2011; Zepp et al., 2012). Act1-mediated K63-linked ubiquitination of TRAF6 is required for NF- $\kappa$ B activation, whereas mRNA stabilizing pathways are dependent on TRAF2/TRAF5. In contrast to this, TRAF4 was demonstrated to inhibit IL-17-induced NF- $\kappa$ B activation via competition for the same binding sites as TRAF6 on Act1, suggesting that TRAF proteins determine downstream specificity of IL-17R-induced Act1-mediated signaling.

In this study, we identified a novel IL-17 signaling cascade via the specific interaction of Act1 with TRAF4 to mediate MEKK3-dependent extracellular signal-regulated kinase 5 (ERK5) activation that is critically important for keratinocyte proliferation and tumor formation. Act1 deficiency in keratinocytes, IL-17RC, or TRAF4 deletion protected mice from IL-17-dependent epidermal proliferation and 7,12-dimethylbenz[a]anthracene (DMBA)/12-O-tetradecanoylphorbol-13-acetate (TPA)-induced carcinogenesis. IL-17-induced IL-17R-Act1-TRAF4-MEKK3-dependent activation of ERK5 resulted in induction of *Steap4* (a metalloredutase for cell metabolism and proliferation). Although knockdown of *Steap4* or *ERK5* diminished IL-17-induced expansion of *p63*<sup>+</sup> epidermal basal cells (*p63*, a transcription factor for the epidermal stem cell proliferation that binds to TRAF4 promoter), overexpression of *p63* induced the expression of TRAF4 in keratinocytes. Importantly, *Steap4*, *p63*, and *TRAF4* were highly expressed in IL-17RC- and Act1-sufficient (but not IL-17RC- or Act1-deficient) skin tumors. *Steap4*, *p63*, and *TRAF4* were also overexpressed in human skin SCC, correlating with the expression of *Il-17a*, formation of Act1-TRAF4-MEKK3 complex, and strong ERK5 activation in the tumors. Collectively,

our data suggest that IL-17-induced *Steap4* might promote a positive feedback on TRAF4 expression via the expansion of *p63*<sup>+</sup> cells, sustaining the activation of the IL-17R-Act1-TRAF4-MEKK3-ERK5 axis for keratinocyte proliferation and tumor formation.

## RESULTS

### Epidermal-specific ablation of IL-17R adaptor Act1 attenuates tumorigenesis

Although several lines of evidence suggest that IL-17-mediated signaling contributes to skin tumorigenesis, the molecular and cellular mechanism remains unclear. The skin cancer model for SCC is initiated by a single application of the carcinogen DMBA to induce a specific point mutation in codon 61 of H-ras and then followed by repeated TPA treatment as a tumor promoter agent for clonal expansion to form papillomas within 10–20 wk, with progression of a portion of the tumors to SCCs within 20–50 wk (Wong et al., 2013). We mostly focused on the analysis of papillomas (treated the mice for 22–23 wk) as we are interested in addressing the role of IL-17 signaling in tumor formation. Nevertheless, some of the tumors developed in our model meet the criteria for SCC in situ and showed atypical squamous proliferation with invasive islands into the dermis, indicative of invasive SCC (Fig. 1 C). After this regimen, mice deficient in IL-17RC or Act1 (the key adaptor of IL-17R) had significantly less tumor formation (Fig. 1, A and B).

Because keratinocytes are highly responsive to IL-17A (Nogales et al., 2008), we hypothesized that IL-17A signaling in the epidermis might play a role in promoting tumorigenesis. To test this hypothesis, we generated epidermis-specific Act1-deficient mice by breeding Act1<sup>fl/fl</sup> mice with the Keratin 5-Cre (K5<sup>Cre</sup>) transgenic line (Crish et al., 2013). Gender- and age-matched K5<sup>Cre</sup>Act1<sup>fl/fl</sup> and K5<sup>Cre</sup>Act1<sup>fl/+</sup> mice (littermate controls) were subjected to the DMBA/TPA regimen. Skin tumor formation occurred in the control mice (K5<sup>Cre</sup>Act1<sup>fl/+</sup>) as early as 5 wk after TPA application, whereas K5<sup>Cre</sup>Act1<sup>fl/fl</sup> mice were strongly resistant to tumor formation (Fig. 1, D and E). The incidence of tumor formation was significantly reduced in the K5<sup>Cre</sup>Act1<sup>fl/fl</sup> mice (Fig. 1 E). These findings suggest that IL-17R-Act1-dependent signaling in the epidermis plays a critical role in skin tumor formation.

Previous studies have shown that DMBA/TPA administration stimulates classic Th17 cells to produce IL-17, which exerts an important role in promoting carcinogenesis-associated inflammation (Wang et al., 2010; He et al., 2012). Consistent with this, we observed increased *Il17a* expression in the skin after TPA administration (Fig. 1 H). Notably, TPA-induced inflammatory gene expression (including *Il6*, *Il11*, *Il1a*, *Il1b*, *Il17a*, *Il17c*, *Il22*, *Ifng*, and *Tnf $\alpha$* ) and inflammatory cell infiltration in the skin were comparable between K5<sup>Cre</sup>Act1<sup>fl/fl</sup> and K5<sup>Cre</sup>Act1<sup>fl/+</sup> mice (Fig. 1, F and H; and not depicted). The tumor-promoting role of IL-17 has been mainly attributed to its proinflammatory properties, by inducing the expression of cytokines like IL-6 to activate the oncogenic STAT3. TPA-induced STAT3 activation was comparable in the skin of

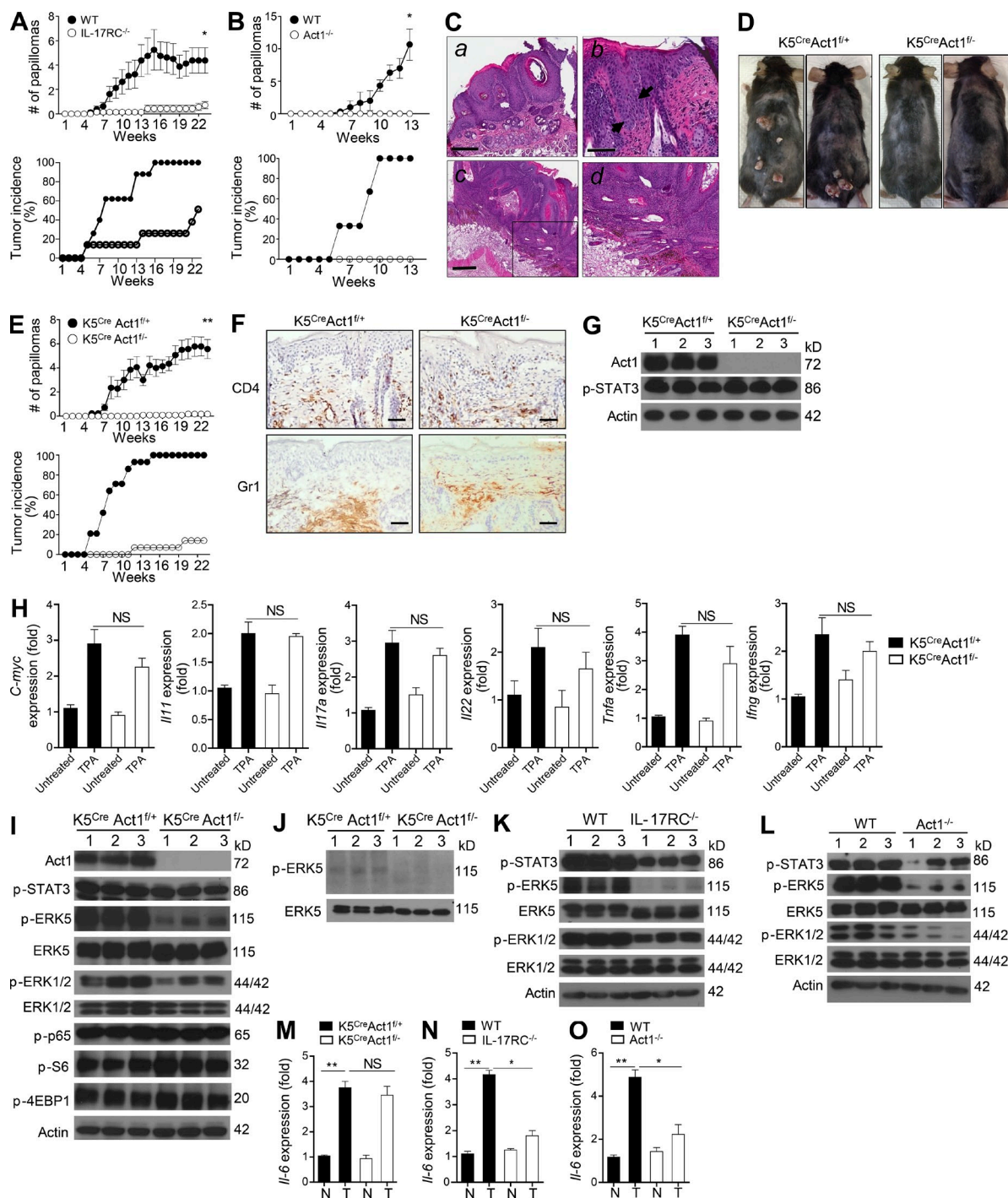


**Figure 1. Keratinocyte-intrinsic IL-17 signaling is required for skin tumor formation.** (A) Tumor numbers and tumor incidence of DMBA/TPA-treated IL-17RC WT and IL-17RC<sup>-/-</sup> mice ( $n = 8$  mice per group). (B) Tumor numbers and tumor incidence of DMBA/TPA-treated Act1 WT and Act1<sup>-/-</sup> mice ( $n = 6$  mice per group). (C) Histological analysis of DMBA/TPA-induced skin tumor in WT mice. (a) Full-thickness squamous dysplasia typical of SCC in situ. (b) Squamous dysplasia with increased mitotic figures (arrows), lack of maturation, and overlying parakeratosis, characteristic of SCC in situ. (c) Atypical squamous proliferation, with invasive islands into the dermis, indicative of invasive SCC. (d) Enlarged view of the indicated frame from c. (D) Photographs of K5<sup>Cre</sup>Act1<sup>fl/-</sup> and K5<sup>Cre</sup>Act1<sup>fl/+</sup> mice treated with DMBA/TPA for 23 wk. (E) Tumor numbers and tumor incidence in DMBA/TPA-treated K5<sup>Cre</sup>Act1<sup>fl/-</sup> and K5<sup>Cre</sup>Act1<sup>fl/+</sup> mice ( $n = 14$  mice per group). (A, B, and E) Tumor numbers presented are the mean number of tumors per mouse  $\pm$  SEM at different time points. \*,  $P < 0.05$ ; \*\*,  $P < 0.01$  (two-way ANOVA). (F) Immunohistochemistry staining for CD4 and Gr1 cells in the TPA-treated skin of K5<sup>Cre</sup>Act1<sup>fl/-</sup> and K5<sup>Cre</sup>Act1<sup>fl/+</sup> mice. Bars: (C, a and c) 300  $\mu$ m; (C, b) 100  $\mu$ m; (F) 50  $\mu$ m. (G) Western blot analysis of epidermal lysates from TPA-treated K5<sup>Cre</sup>Act1<sup>fl/-</sup> and K5<sup>Cre</sup>Act1<sup>fl/+</sup> mice. Each lane represents an individual sample. (H) Gene expression analysis from the skin of

K5<sup>Cre</sup>Act1<sup>fl/-</sup> compared with that of K5<sup>Cre</sup>Act1<sup>fl/+</sup> mice (Fig. 1 G), while IL-6 levels and phosphorylation of STAT3 and p65 (NF-κB) were also comparable between the Act1-sufficient and -deficient tumors (Fig. 1, I and M). Instead, ERK5, and to a lesser extent ERK1/2, activation (but not JNK, p38, or mTOR activation [as indicated by the phosphorylated S6 and 4EBP1]) was reduced in the tumors from K5<sup>Cre</sup>Act1<sup>fl/-</sup> mice compared with those from the control mice (Fig. 1, I and J; and not depicted). These results suggest that the loss of IL-17 signaling specifically in the epidermis resulted in a defect in ERK activation, implicating ERKs in IL-17-Act1-dependent skin tumorigenesis. In support of this, ERK activation was also dramatically reduced in tumors from IL-17RC and Act1 complete knockout mice compared with that in the control mice (Fig. 1, K and L). Nevertheless, it is important to note that, in addition to reduction of ERK1/2 and ERK5 activation, IL-6 levels and STAT3 activation were also reduced in tumors from IL-17RC and Act1 complete knockout mice, indicating IL-17 signaling in cellular compartments other than epidermis probably contributes to IL-6 production to impact tumorigenesis as well (Fig. 1, K, L, N, and O).

#### IL-17A activates the MEKK3-ERK5 pathway to drive epidermal proliferation

Epidermal-specific Act1 deficiency resulted in significantly reduced epidermal hyperplasia and BrdU incorporation in the epidermis after treatments with TPA or IL-17A (Fig. 2, A-D), implicating the critical role of keratinocyte-intrinsic IL-17 signaling in promoting cell proliferation/survival. TPA application on mice deficient in IL-17RC also resulted in decreased epidermal thickening compared with the WT controls (not depicted). Moreover, ex vivo culture of keratinocytes with IL-17A resulted in more BrdU incorporation, increased total cell counts, and enhanced expression of *c-myc* and *Cyclin D1* compared with the untreated cells (Fig. 2, E-G). Collectively, these data indicate that IL-17A indeed acts directly on keratinocytes to induce proliferation, resulting in epidermal hyperplasia. Although IL-17-induced IL-6 expression (see Fig. 5 A) was implicated in promoting cell growth, anti-IL-6 neutralizing antibody failed to block IL-17A-induced cell proliferation in primary keratinocytes (Fig. 2, E and G; Riedemann et al., 2003; Rochman et al., 2005; Yen et al., 2006), whereas this antibody was able to inhibit IL-6-induced STAT3 phosphorylation in these cells (Fig. 2 E). These results suggest that the observed IL-17-induced keratinocyte proliferation was probably independent of IL-6.

Because epidermal-specific Act1 deficiency did not diminish TPA-induced STAT3 activation, it is important to identify the signaling mechanism for IL-17-mediated epidermal proliferative response. Previous studies have shown that IL-17 activates multiple intracellular signaling pathways, including NF-κB and MAPKs such as p38, JNK, and ERK1/2 (Mauro et al., 2003; Chang et al., 2006; Qian et al., 2007; Wang et al., 2013). Considering the dramatic reduction of ERK5 activation in IL-17RC- and Act1-deficient tumors (Fig. 1, I, K, and L), we decided to investigate the ERK5 pathway, which has been shown to play a crucial role in cell proliferation and skin tumorigenesis in both mice and human (Deschênes-Simard et al., 2014; Finegan et al., 2015). Western blot analysis revealed that intradermal IL-17A injection indeed resulted in sustained activation of ERK5, indicated by its phosphorylation, whereas the activation of ERK1/2 was transient (Fig. 3 A). Interestingly, intradermal injection of IL-17A in the presence of ERK5 siRNA (75% reduction of ERK5 expression in the epidermis) resulted in less epidermal thickening compared with IL-17A injection with control siRNA (Fig. 3 B), suggesting the importance of the ERK5 pathway in IL-17A-mediated Act1-dependent proliferation. In support of this, intradermal injection of IL-17A in the presence of MEK5 inhibitor (Bix 02189), which blocks ERK5 activation (Tatake et al., 2008), also resulted in less epidermal thickening compared with IL-17A injection alone (Fig. 3 B).

To investigate IL-17-mediated signaling mechanism in keratinocytes, we isolated primary keratinocytes from WT or Act1-deficient newborn pups. In addition to Act1-dependent activation of NF-κB (indicated by phosphorylated IκBα), p38, and ERK1/2, IL-17A stimulation induced sustained activation of ERK5 in keratinocytes (Fig. 3 C), which was abolished in Act1-deficient cells. ERK5, also known as big MAPK, is the least studied of the MAPKs (Nithianandarajah-Jones et al., 2012). It is activated by the upstream MEK5, which is activated by the MEKK2 or MEKK3. This MEKK2/3-MEK5-ERK5 pathway has been shown to be important in cell survival and proliferation and is involved in various cancers such as breast and prostate (Castro and Lange, 2010; Drew et al., 2012). We found that Act1 immunoprecipitated with MEKK3 (but not MEKK2) upon overexpression, as well as in response to stimulation with IL-17A, implicating MEKK3 as a component in the IL-17A signaling cascade and a potential upstream kinase for ERK5 activation (Fig. 3, D-F; and not depicted). Furthermore, IL-17A induced interaction of MEKK3 with MEK5 as well as ERK5, and this interaction

TPA-treated K5<sup>Cre</sup>Act1<sup>fl/-</sup> and K5<sup>Cre</sup>Act1<sup>fl/+</sup> mice graphed as relative fold over untreated (mean and SEM were derived from biological replicates, *n* = 3). (I) Western blot analysis of the tumor tissue from DMBA/TPA-treated K5<sup>Cre</sup>Act1<sup>fl/-</sup> and K5<sup>Cre</sup>Act1<sup>fl/+</sup> mice. (J) Immunoprecipitation of ERK5 with anti-ERK5, followed by Western blot analysis with anti-pERK5 using lysates of individual tumors from K5<sup>Cre</sup>Act1<sup>fl/-</sup> and K5<sup>Cre</sup>Act1<sup>fl/+</sup> mice treated with DMBA/TPA. (K and L) Western blot analysis of the tumor tissue from DMBA/TPA-treated IL-17RC WT and IL-17RC<sup>-/-</sup> mice (K) and Act1 WT and Act1<sup>-/-</sup> mice (L). Each lane represents an independent sample. (M-O) *Il6* expression analysis from nontumor (N) or tumor (T) samples of K5<sup>Cre</sup>Act1<sup>fl/-</sup> and K5<sup>Cre</sup>Act1<sup>fl/+</sup> mice (M), IL-17RC WT and IL-17RC<sup>-/-</sup> mice (N), and Act1 WT and Act1<sup>-/-</sup> mice (O) harvested at the end of DMBA/TPA treatment. Gene expression is graphed as mean fold induction of tumor over nontumor ± SEM. SEM was derived from biological replicates (*n* = 3 samples from independent mice). Data are representative of at least three experiments. \*, *P* < 0.05; \*\*, *P* < 0.01.

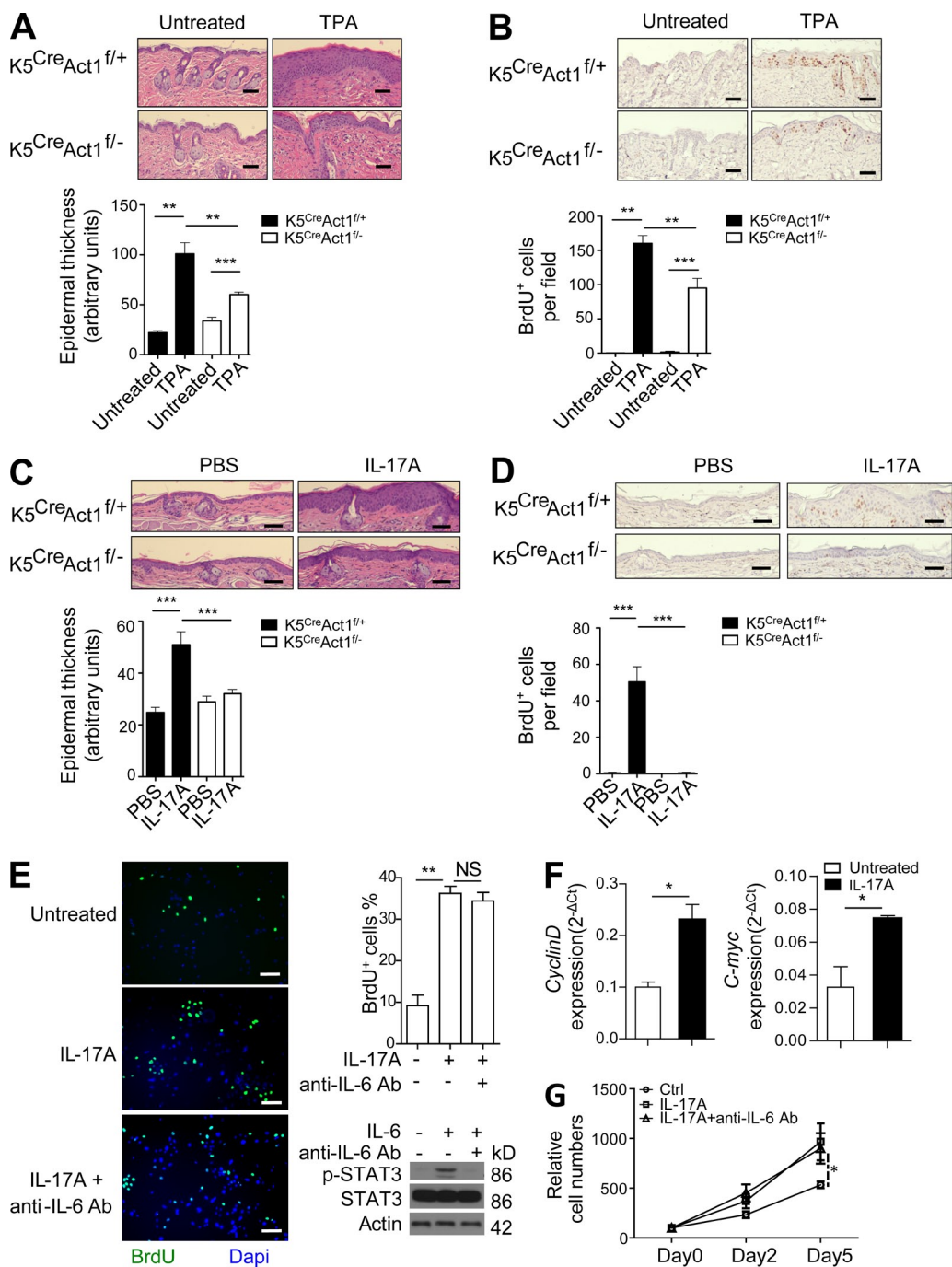


**Figure 2. IL-17 stimulation induces keratinocyte proliferation.** (A) H&E staining of TPA-treated K5<sup>Cre</sup>Act1<sup>f/-</sup> and K5<sup>Cre</sup>Act1<sup>f/+</sup> mice. (B) BrdU staining in mice treated as in A, with BrdU (100  $\mu$ g per mouse) injected 24 h before tissue collection. (C) Ears of K5<sup>Cre</sup>Act1<sup>f/-</sup> and K5<sup>Cre</sup>Act1<sup>f/+</sup> mice were injected intradermally either with IL-17A in PBS or PBS alone. H&E staining of PBS or IL-17A-injected ear sections of K5<sup>Cre</sup>Act1<sup>f/-</sup> and K5<sup>Cre</sup>Act1<sup>f/+</sup> mice. (A and C) Graphs represent mean epidermal thickness in arbitrary units  $\pm$  SEM. (D) BrdU staining of PBS or IL-17A-injected ear section of K5<sup>Cre</sup>Act1<sup>f/-</sup> and K5<sup>Cre</sup>Act1<sup>f/+</sup> mice. (B and D) Graphs represent mean BrdU<sup>+</sup> cells per 10 $\times$  magnification field  $\pm$  SEM. (E) Serum-starved primary keratinocytes left untreated or treated with IL-17A or IL-17A + 2  $\mu$ g/ml anti-IL-6 neutralizing antibody for 24 h, with BrdU added during the last 2 h. Graph represents mean percentage of BrdU<sup>+</sup> cells per 10 $\times$  magnification field  $\pm$  SEM. Western blot with the indicated antibodies using lysates from keratinocytes untreated or treated with IL-6 (50 ng/ml, 30 min) with or without the presence of 2  $\mu$ g/ml IL-6 neutralizing antibody. Bars: (A–D) 50  $\mu$ m; (E) 100  $\mu$ m. (F) Gene expression of *Cyclin D* and *c-myc* in primary keratinocytes left untreated or treated with IL-17A  $\pm$  SEM. (G) Primary keratinocytes left untreated or treated with IL-17A or IL-17A + 2  $\mu$ g/ml anti-IL-6 neutralizing antibody for the indicated days, followed by counting of cells total cell numbers. Three replicates for each time point  $\pm$  SEM are shown. For imaging analysis, five fields were analyzed. All the data are representative of at least three experiments. \*,  $P < 0.05$ ; \*\*,  $P < 0.01$ ; \*\*\*,  $P < 0.001$ .

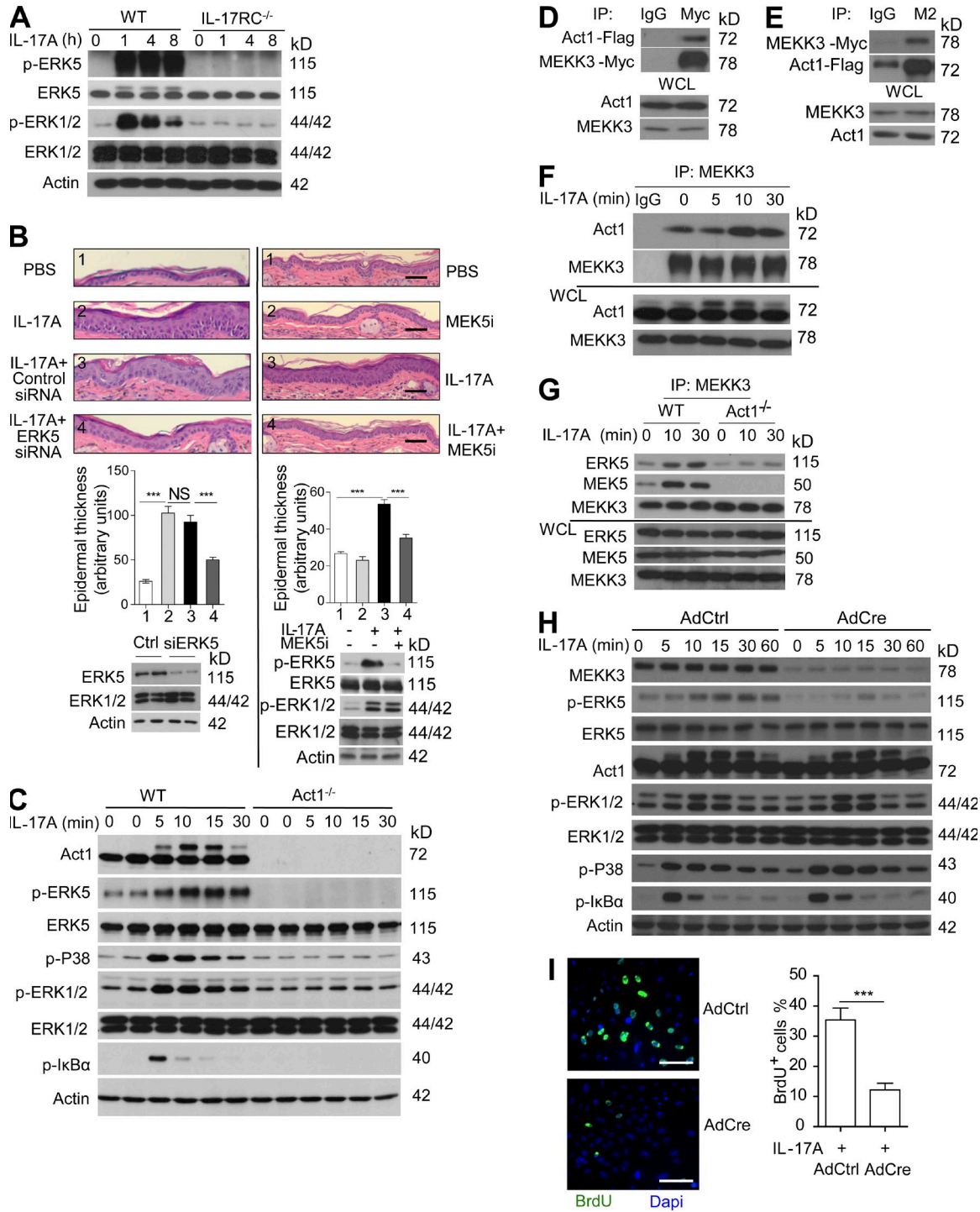


**Figure 3. The MEKK3-ERK5 axis is critical for IL-17-induced epidermal keratinocyte proliferation.** (A) Western blot analysis of epidermal lysates from ears of WT and IL-17RC<sup>-/-</sup> mice injected with IL-17A for the indicated times. (B) H&E staining of ear sections of C57BL/6 WT mice injected with PBS, IL-17A in the presence or absence of ERK5 siRNA (left), or MEK5 inhibitor Bix 02189 (right). Graphs represent mean epidermal thickness (a.u.) ± SEM. \*\*\*, P < 0.001 (Student's *t* test, five fields were analyzed; *n* = 5 mice per group). Western blots were performed to show ERK5 siRNA efficacy and MEK5 inhibitor specificity in vivo. Epidermal lysates from C57BL/6 WT mice 48 h after injection with control siRNA and ERK5 siRNA were subjected to Western blotting with antibodies against ERK5, ERK1/2, and actin to show the ERK5 knockdown efficiency. Each lane represents one independent sample. Likewise, epidermal lysates from WT C57/B6 WT mice 8 h after injection with PBS, IL-17A, and IL-17A + Bix 02189 were subjected to Western blotting with antibodies to show MEK5 inhibitor specificity in vivo. (C) Western blot analysis of primary keratinocytes isolated from Act1 WT or Act1<sup>-/-</sup> mice and stimulated with 100 ng/ml IL-17A for the indicated times. Data are representative of three independent experiments. (D and E) HeLa cells were transiently cotransfected with Flag-tagged mouse Act1 and Myc-tagged MEKK3. Lysates of transfected cells were subjected to immunoprecipitation with anti-Myc

was abolished in Act1-deficient cells (Fig. 3 G). To study the role of MEKK3 in IL-17A signaling, we generated MEKK3-deficient cells by infecting MEKK3<sup>fl/fl</sup> keratinocytes with adenovirus expressing Cre recombinase (Fig. 3 H). IL-17A-dependent ERK5 activation was indeed dependent on MEKK3, whereas the activation of NF- $\kappa$ B, p38, and ERK1/2 were not (Fig. 3 H). Consistently, IL-17A-induced proliferation was substantially reduced in MEKK3<sup>-/-</sup> keratinocytes (Fig. 3 I).

#### TRAF4 bridges Act1 with MEKK3-ERK5 to promote IL-17A-induced keratinocyte proliferation

The specificity of downstream signaling pathways from IL-17R seems to be determined by the interaction of Act1 with different TRAF molecules. For instance, Act1-TRAF6 is critical for NF- $\kappa$ B activity for inflammatory gene expression, whereas Act1-TRAF2/TRAF5 complex formation is essential for IL-17A to stabilize proinflammatory mRNAs (Hartupee et al., 2009; Bulek et al., 2011; Sun et al., 2011). Although MEKK3 is a critical player in IL-17A-induced Act1-mediated ERK5 activation, we sought to determine whether TRAF molecules might serve as intermediates to link Act1 to MEKK3. Screening through the TRAFs, we found that Act1 and MEKK3 (but not MEKK2) form a complex with TRAF4 upon IL-17A stimulation (Fig. 4 A and not depicted) and TRAF4 is required for IL-17A-induced interaction of Act1 with MEKK3 (Fig. 4 B). More importantly, TRAF4 was specifically necessary for IL-17A-induced ERK5 activation, whereas ERK1/2, p38, JNK, and NF- $\kappa$ B activation were not abolished but were rather enhanced in the absence of TRAF4 (Fig. 4 C; Zepp et al., 2012). Based on these results, we concluded that TRAF4 is a critical adaptor that links Act1 to the MEKK3-MEK5-ERK5 pathway for IL-17A-induced ERK5 activation.

Importantly, TRAF4 deficiency substantially diminished IL-17A-induced ERK5 activation and epidermal hyperplasia (Fig. 4, D and E), suggesting the importance of the TRAF4-dependent pathway in IL-17-Act1-mediated proliferation. We then subjected the gender- and age-matched TRAF4<sup>-/-</sup> and control mice (littermate controls) to the DMBA/TPA skin cancer model. The tumor numbers and tumor incidence were substantially reduced in TRAF4<sup>-/-</sup> mice as compared with that in the control mice (Fig. 4, F and G), indicating that the TRAF4-dependent signaling is also critical for tumor formation. Interestingly, we noted that during the treatment of TPA, especially from 6 to 14 wk, some of the TRAF4<sup>-/-</sup> mice developed some tiny bumps that went away within 1–2 wk. Consistent with the impact of Act1 deficiency, phosphorylation of STAT3 and p65 (NF- $\kappa$ B) was also comparable between

the TRAF4-sufficient and -deficient tumors. In contrast, ERK5 activation was greatly reduced in the tumors from TRAF4<sup>-/-</sup> mice compared with those from the control mice (Fig. 4 H). Collectively, these results suggest that the loss of TRAF4 signaling resulted in a defect in IL-17-induced ERK5 activation (Fig. 4, C and D), which probably contributes to IL-17-Act1-dependent cell proliferation (Fig. 4 E) and skin tumorigenesis (Fig. 4, F–H).

#### Steap4 is critical for IL-17A-induced TRAF4-MEKK3-ERK5-mediated epidermal proliferation

We next explored the question regarding how IL-17A mediates epidermal proliferation through the IL-17R-Act1-TRAF4-MEKK3-ERK5 pathway. Although ERK5 has been directly implicated in cell proliferation, IL-17A moderately induced the expression of *c-myc*, a known ERK5 target gene in cultured keratinocytes in an IL-17RC-, Act1-, ERK5-, MEKK3-, and TRAF4-dependent manner (Fig. 5, A–E). In an independent array analysis in kidney and colon epithelial cells, we identified several novel IL-17-induced genes involved in cell proliferation. Through extensive screening, we decided to focus on *Steap4*, a metalloredoxase with NADPH oxidase (NOX) activity that plays a role in cell metabolism but has also been shown to be associated with prostate cancer (Korkmaz et al., 2005; Wellen et al., 2007; ten Freyhaus et al., 2012; Gauss et al., 2013). We found that IL-17A stimulation resulted in strong up-regulation of *Steap4* in keratinocytes. IL-17A-induced *Steap4* expression was abolished in IL-17RC- and Act1-deficient cells and substantially reduced in MEKK3-, TRAF4-, and ERK5-deficient keratinocytes (Fig. 5, A–E). These results strongly indicate that *c-myc* and *Steap4* are target genes of the IL-17R-Act1-TRAF4-MEKK3-ERK5 axis. Consistently, *c-myc* and *Steap4* were induced in IL-17A-injected skin, but the expression of these genes was suppressed when IL-17A was coinjected with ERK5 siRNA (Figs. 5 F and 3 B). Consistently, MEK5 inhibitor (Bix 02189) also blocked *c-myc* and *Steap4* induction in IL-17A-injected skin (Fig. 5 G). TRAF4 deficiency also greatly reduced the induction of *c-myc* and *Steap4* in the IL-17A-injected skin tissue, accompanied by loss of ERK5 activation (Figs. 5 H and 4 D). It is important to note that although IL-17A-induced expression of proinflammatory cytokines such as *Cxcl1* and *IL-6* in keratinocytes was dependent on IL-17RC and Act1, they were not affected by MEKK3 or ERK5 deficiency (Fig. 5, A–H). Moreover, consistent with the inhibitory role of TRAF4 in IL-17A-induced NF- $\kappa$ B activation, IL-17A-induced *IL-6* and

(D) or anti-Flag (M2; E) antibodies, followed by Western blot analysis. (F) HeLa cells were treated with IL-17A, and lysates were immunoprecipitated with anti-MEKK3, followed by Western blot analysis. (G) Act1 WT and Act1<sup>-/-</sup> kidney epithelial cells were treated with IL-17A for the indicated times. Lysates were immunoprecipitated with anti-MEKK3 antibody, followed by Western blot analysis. (H) Primary keratinocytes were isolated from MEKK3<sup>fl/fl</sup> mice, followed by infection with adenovirus encoding Cre-recombinase or empty vector. Cells were then stimulated with IL-17A, followed by Western blot analysis. (I) BrdU incorporation of serum-starved MEKK3-deficient keratinocytes (as described in H) treated with IL-17A for 24 h, with 10  $\mu$ M BrdU added during the last 2 h. Graph represents mean percentage of BrdU<sup>+</sup> cells per field ( $n = 5$  fields)  $\pm$  SEM. \*\*\*,  $P < 0.001$  (Student's *t* test). Bars: (B) 50  $\mu$ m; (I) 100  $\mu$ m. All the data are representative of at least three experiments.

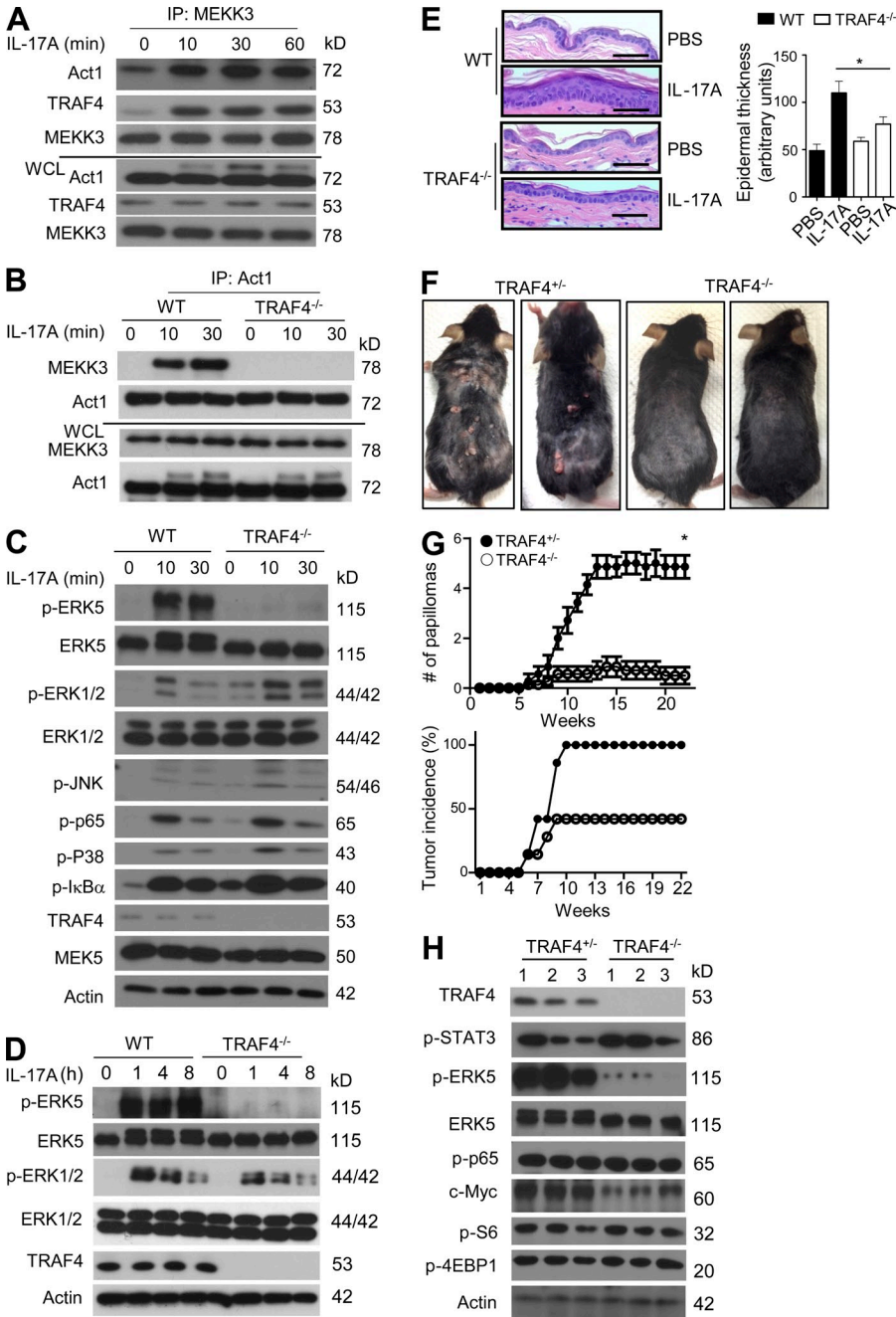


**Figure 4. TRAF4 is a bridge protein for the Act1-mediated MEKK3-ERK5 pathway.** (A) WT kidney epithelial cells were treated with IL-17A for the indicated times. Lysates were then immunoprecipitated with anti-MEKK3 antibody, followed by Western blot analysis. (B) TRAF4 WT and TRAF4<sup>-/-</sup> kidney epithelial cells were treated with IL-17A for the indicated times. Cell lysates were then immunoprecipitated with anti-Act1 antibody, followed by Western blot analysis. (C) TRAF4 WT and TRAF4<sup>-/-</sup> primary keratinocytes were treated with IL-17A, followed by Western blot analysis. (D) Western blot analysis of epidermal lysates from ears of WT and TRAF4<sup>-/-</sup> mice injected with IL-17A for the indicated times. (E) H&E staining of ear sections from TRAF4 WT or TRAF4<sup>-/-</sup> mice injected intradermally with IL-17A or PBS alone. Graph represents mean epidermal thickness (arbitrary units) ± SEM. \*, P < 0.05 (five fields were analyzed, Student's *t* test). Bars, 50 μm. (F) Photographs of TRAF4<sup>+/-</sup> and TRAF4<sup>-/-</sup> mice treated with DMBA/TPA for 22 wk. (G) Tumor numbers and tumor incidence of DMBA/TPA-treated TRAF4<sup>+/-</sup> and TRAF4<sup>-/-</sup> mice (*n* = 7 mice per group). Tumor numbers presented are the mean number of tumors per mice ± SEM at different time points. \*, P < 0.05 (two-way ANOVA). (H) Western blot analysis of the tumor tissue from TRAF4<sup>+/-</sup> and TRAF4<sup>-/-</sup> mice. Each lane represents an independent sample. All experimental data were verified in at least three independent experiments.

*CXCL1* levels were actually slightly enhanced in TRAF4-deficient keratinocytes compared with that in WT cells (Fig. 5 D).

Although the Act1-TRAF4-MEKK3-ERK5 axis is required for IL-17A-induced epidermal proliferation, our results also demonstrated that *Steap4* is a major target gene of this pathway. Because *Steap4*, a metalloredoxase with NOX activity, has been implicated in promoting cell metabolism and proliferation, we then tested the importance of *Steap4* in IL-17A-induced epidermal proliferation. When IL-17A was coinjected with *Steap4* siRNA, IL-17A-induced epidermal hyperplasia was substantially reduced compared with that

injected with control siRNA (Fig. 5 I). Consistently, whereas IL-17A-induced *c-myc* expression was decreased in *Steap4* knockdown skin tissue, inflammatory gene expression (*CXCL1* and *IL-6*) was not affected by *Steap4* siRNA injection (Fig. 5, J and K). It is intriguing to note that IL-17A-induced ERK5 activation was reduced in *Steap4* knockdown skin tissue compared with that injected with control siRNA (Fig. 5 K). Collectively, these results suggest that IL-17A-induced *Steap4* expression plays a critical role in the epidermal proliferative response triggered by IL-17A stimulation, possibly by sustaining ERK5 activation and *c-myc* expression.

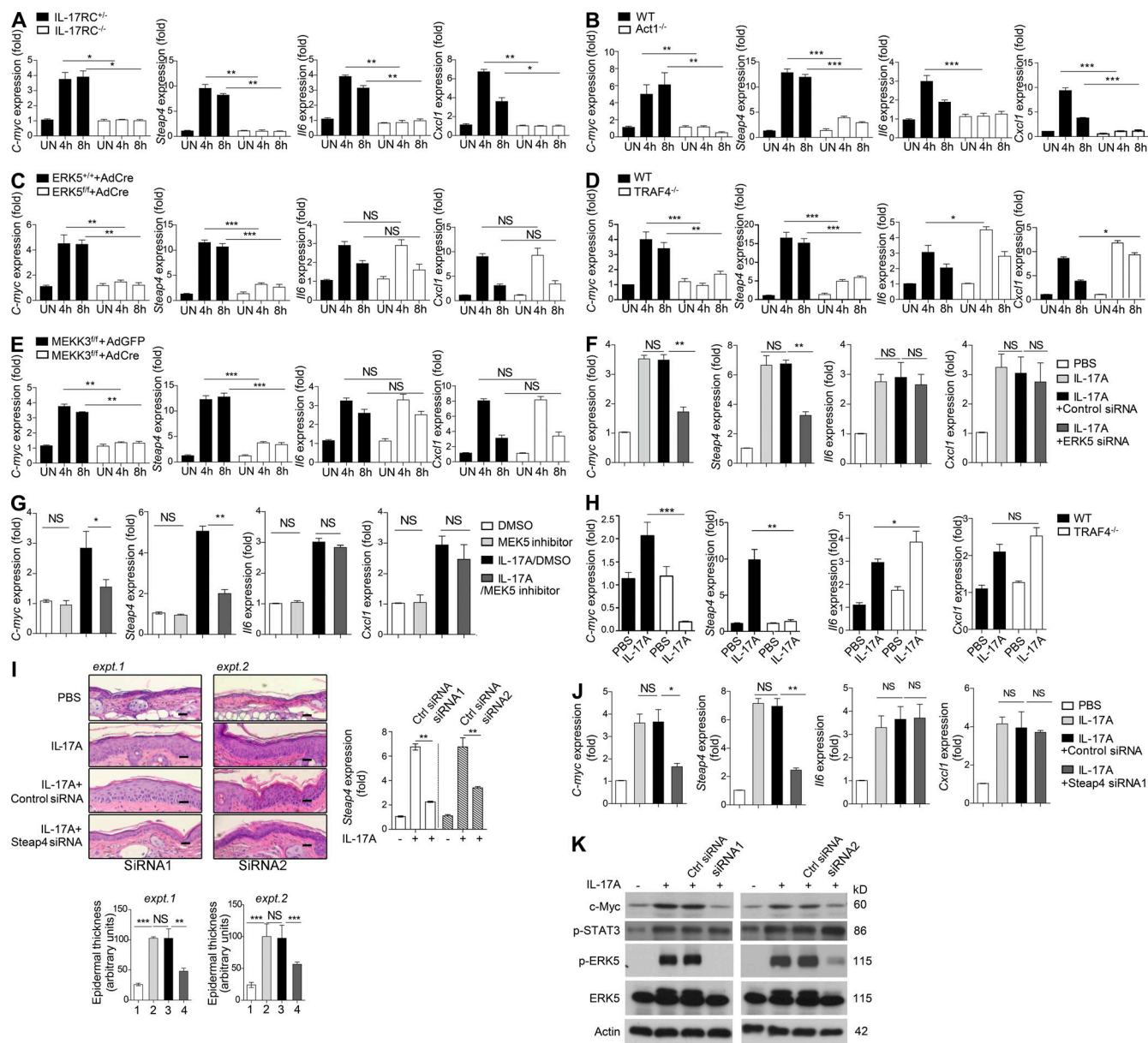


**Figure 5. The Act1-ERK5 axis mediates critical IL-17 target genes for keratinocyte proliferation.** (A) Primary keratinocytes isolated from IL-17RC<sup>+/+</sup> or IL-17RC<sup>-/-</sup> mice were stimulated with IL-17A for the indicated times, followed by RT-PCR analysis. (B) Primary keratinocytes isolated from Act1 WT or Act1<sup>-/-</sup> mice were stimulated with IL-17A for the indicated times, followed by RT-PCR analysis. (C) Primary keratinocytes isolated from ERK5<sup>+/+</sup> and ERK5<sup>fl/fl</sup> mice were infected with Cre-encoding adenovirus for 48 h before stimulation. Cells were then stimulated with IL-17A for the indicated times, followed by RT-PCR analysis. (D) Primary keratinocytes isolated from TRAF4 WT or TRAF4<sup>-/-</sup> mice were stimulated with IL-17A for the indicated times, followed by RT-PCR analysis. (E) Primary keratinocytes isolated from MEK3<sup>fl/fl</sup> mice were infected with either Cre-encoding (AdCre) or empty adenovirus (AdGFP) for 48 h before stimulation. Cells were then stimulated with IL-17A for the indicated times, followed by RT-PCR analysis. (A-E) Gene expression is graphed as mean fold induction over untreated  $\pm$  SEM. SEM was derived from three technical replicates. Data are representative of at least two independent experiments. (F and G) RNA isolated from the ear tissue of mice (with the same treatments as described in Fig. 3 B) was subjected to RT-PCR analysis. Gene expression is graphed as mean fold induction over PBS  $\pm$  SEM. (H) RT-PCR analysis of the indicated genes isolated from the ear tissue of TRAF4 WT or TRAF4<sup>-/-</sup> mice injected with PBS or IL-17A. Gene expression is graphed as mean fold induction over PBS treated  $\pm$  SEM. (F-H) SEM was derived from biological replicates ( $n = 5$  mice). (I) H&E staining of ear skin sections from WT mice injected with PBS, IL-17A, IL-17A + control siRNA, or IL-17A + Steap4 siRNA ( $n = 5$  mice each group). Bars, 50  $\mu$ m. Graphs represent mean epidermal thickness (a.u.)  $\pm$  SEM and were derived from five fields. Steap4 siRNA1 and Steap4 siRNA2 were used in experiments 1 and 2, respectively. Graph on the right shows RT-PCR analysis of Steap4 mRNA levels in the ear epidermis after IL-17A coinjection with control and Steap4 siRNA. (J) RNA isolated from the ear tissue of mice treated as in H using Steap4 siRNA1 was subjected to RT-PCR analysis. Gene expression is graphed as mean fold induction over PBS treated  $\pm$  SEM. SEM was derived from biological replicates ( $n = 5$  mice). (K) Western blot analysis of homogenized epidermal samples described in I. Student's  $t$  test was used for all statistical analysis: \*,  $P < 0.05$ ; \*\*,  $P < 0.01$ ; \*\*\*,  $P < 0.001$ . All the data are representative of different independent experiments as described above.

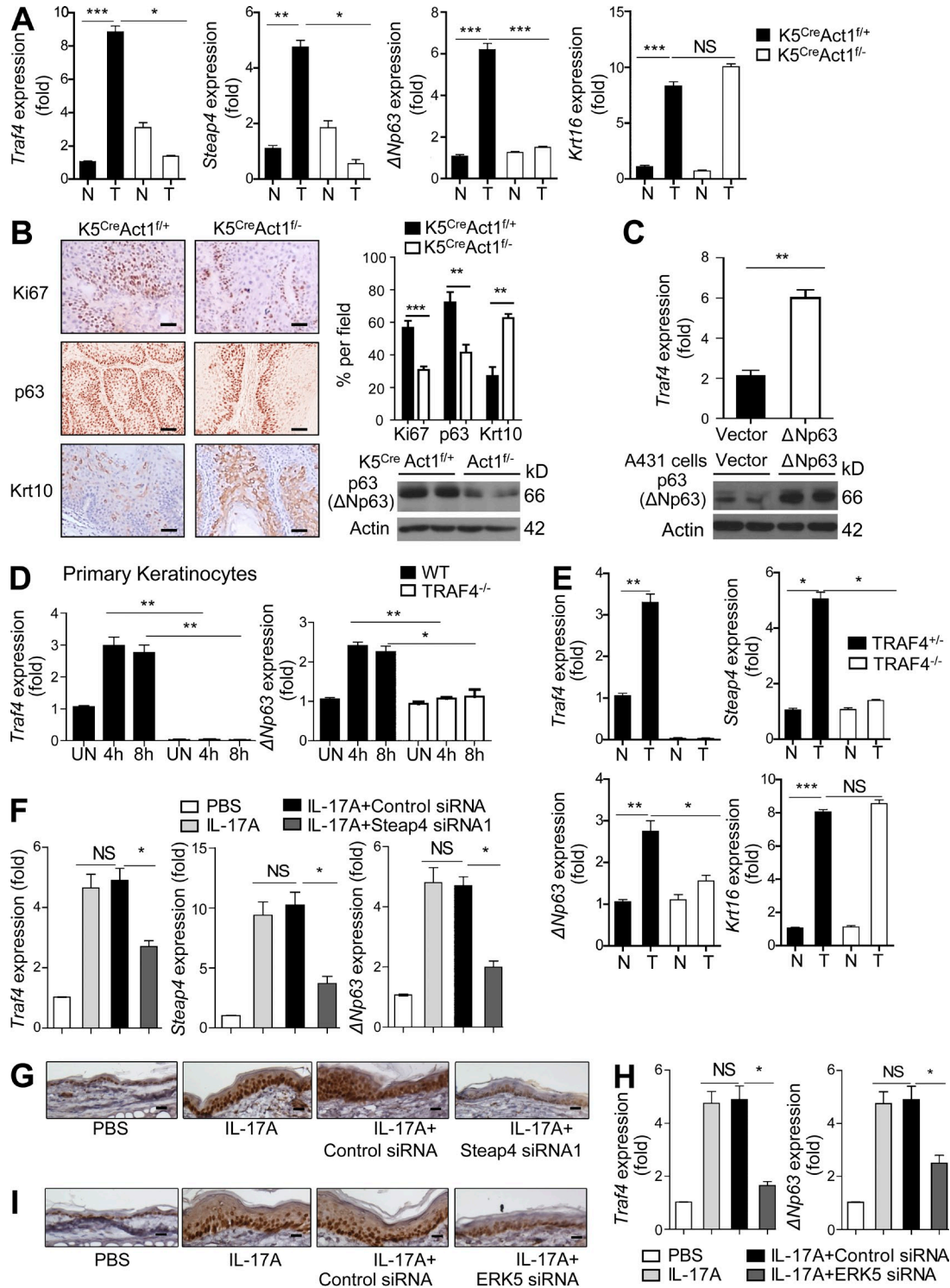


**Figure 6. IL-17A drives Steap4-mediated positive feedback on TRAF4 expression via expansion of ΔNp63<sup>+</sup> basal cells.** (A) RT-PCR analysis from nontumor (N) or tumor (T) samples of K5<sup>Cre</sup>Act1<sup>fl/-</sup> and K5<sup>Cre</sup>Act1<sup>fl/+</sup> mice at 23 wk of DMBA/TPA treatment. Gene expression is graphed as mean fold of tumor over nontumor ± SEM. Data shown are representative of three independent experiments. (B) Immunohistochemistry staining of tumor tissue from K5<sup>Cre</sup>Act1<sup>fl/-</sup> or K5<sup>Cre</sup>Act1<sup>fl/+</sup> mice for Ki67, p63, and Krt10. Graph represents mean percentage of Ki67, p63, and Krt10<sup>+</sup> cells per field (n = 5) ± SEM. Western blot shows representative ΔNp63 expression levels in tumor tissues from DMBA/TPA-treated K5<sup>Cre</sup>Act1<sup>fl/-</sup> or K5<sup>Cre</sup>Act1<sup>fl/+</sup> mice. Data are representative of three experiments. (C) Human A431 keratinocytes were transfected with ΔNp63 or empty vector. 36 h after transfection, levels of TRAF4 transcripts and ΔNp63 protein were analyzed by RT-PCR and Western blot. Traf4 expression is graphed as relative mean fold induction ± SEM. SEM was derived from three technical replicates. (D) Primary keratinocytes isolated from TRAF4 WT or TRAF4<sup>-/-</sup> mice were stimulated with IL-17A for the indicated

### IL-17A drives Steap4-mediated positive feedback on TRAF4 expression

ERK5 activation was greatly reduced in the tumors from IL-17RC<sup>-/-</sup>, Act1<sup>-/-</sup>, K5<sup>Cre</sup>Act1<sup>f/f</sup>, and TRAF4<sup>-/-</sup> mice compared with those from their control mice (Fig. 1, I, K, and M; and Fig. 4 H). The question was then how this IL-17R-Act1-TRAF4-dependent ERK5 pathway becomes a dominant pathway in the epidermis to promote cell proliferation and tumorigenesis. Notably, *Traf4* and *Steap4* expression was highly induced in the tumors from IL-17RC WT, Act1 WT, and K5<sup>Cre</sup>Act1<sup>f/+</sup> mice but not in the IL-17RC<sup>-/-</sup>, Act1<sup>-/-</sup>, or K5<sup>Cre</sup>Act1<sup>f/-</sup> tumors (Fig. 6 A and not depicted). Furthermore, because it was reported that transcription factor p63 (a master regulator of epidermal stem cell proliferation) binds to the TRAF4 promoter and up-regulates its transcription (Gu et al., 2007), we also examined p63 levels in the tumors. The *p63* locus is expressed as multiple isoforms, most notably through two promoters that produce N-terminal variants either containing or lacking the p53-like transactivation domain (TAp63 or ΔNp63, respectively; DeYoung and Ellisen, 2007). The major p63 isoform expressed in stratified squamous epithelium and SCC is ΔNp63α (Ihrle et al., 2005; Rocco et al., 2006). We found that p63 (isoform ΔNp63) expression and p63<sup>+</sup> cells were highly enhanced in the tumor tissue from the IL-17RC WT, Act1 WT, and K5<sup>Cre</sup>Act1<sup>f/+</sup> mice compared with the IL-17RC<sup>-/-</sup>, Act1<sup>-/-</sup>, and K5<sup>Cre</sup>Act1<sup>f/-</sup> tumor tissues, respectively (Fig. 6, A and B; and not depicted). In contrast, IL-17RC- and Act1-sufficient tumor tissue expresses less Keratin 10 (Krt10) than the IL-17RC- and Act1-deficient tumor tissue, indicating that IL-17R-Act1 might simultaneously down-regulate markers associated with keratinocyte differentiation (Nogales et al., 2008). Concomitantly, there was more staining for the proliferative marker Ki67<sup>+</sup> in the tumor tissue from K5<sup>Cre</sup>Act1<sup>f/+</sup> mice than in the tissue from K5<sup>Cre</sup>Act1<sup>f/-</sup> mice (Fig. 6 B).

We found that overexpression of p63 (isoform ΔNp63) indeed induced TRAF4 expression, validating the p63-driven transcriptional activation of TRAF4 (Fig. 6 C). Notably, the expression levels of *Steap4* and p63 (isoform ΔNp63) were much lower in the TRAF4-deficient tumors compared with that in TRAF4-sufficient tumors (Fig. 6 E). These results suggest that the TRAF4-dependent pathway is reciprocally required for the up-regulation of p63 in the tumor tissues. In searching for the mechanism for how TRAF4 reciprocally impacts p63 expression, we found that IL-17A stimulation was able to induce the expression of p63 (isoform ΔNp63)

and TRAF4 in keratinocytes and IL-17A injection induced the expansion of p63<sup>+</sup> basal cells in the epidermis (Fig. 6, D and G). Importantly, IL-17A-induced expression of p63 (isoform ΔNp63) and TRAF4 and the expansion of p63<sup>+</sup> basal cells were substantially reduced in *Steap4* and ERK5 knockdown skin tissues (Fig. 6, F-I). These results suggest the critical role of *Steap4* in IL-17A-driven induction of p63 and TRAF4, providing a positive feedback loop for the IL-17A-induced TRAF4-dependent pathway. As shown in Fig. 5 (H and I), IL-17A-induced ERK5 activation and *c-myc* expression were indeed reduced in *Steap4* knockdown skin tissue compared with that injected with control siRNA. Collectively, our data suggest that the IL-17R-Act1-induced *Steap4* might promote a positive feedback on TRAF4 expression via the expansion of p63<sup>+</sup> cells, sustaining activation of the IL-17R-Act1-TRAF4-MEKK3-ERK5 axis for IL-17A-induced keratinocyte proliferation and tumor formation.

### TRAF4-ERK5 is hyperactivated in human skin SCC

TRAF4 and p63 have long been found to be overexpressed in various carcinomas (Rocco et al., 2006; Camilleri-Broët et al., 2007), whereas *Steap4* has been shown to be associated with prostate cancer (Korkmaz et al., 2005). We indeed found that *Steap4*, *p63* (isoform ΔNp63), and *Traf4* were overexpressed at both RNA and proteins levels in human skin SCC samples compared with normal skin tissue (Fig. 7, A-D). Importantly, the overexpression of TRAF4 strongly correlated with p-ERK5 activation and expression levels of *Steap4* and *p63* (Fig. 7, C and D). It is intriguing to note that Act1 expression was also highly elevated and even modified in human skin SCC samples compared with normal skin tissue (Fig. 7 D). Importantly, coimmunoprecipitation experiments showed that the Act1-MEKK3-TRAF4 complex was readily detectable in the SCC lysates but not in normal skin tissue, indicating activation of the Act1-TRAF4-dependent pathway (Fig. 7 E). Notably, IL-17A levels correlated with TRAF4 expression in SCC, implicating IL-17A signaling in the SCC with overexpression of TRAF4 (Fig. 7 A). Collectively, our data imply that the emergence of IL-17A and TRAF4 allows IL-17R-Act1 to fully engage the MEKK3-ERK5 axis, promoting tumor formation through the induction of genes critical for cell proliferation.

### DISCUSSION

IL-17A is emerging as an important cytokine in cancer promotion and progression. This study discovered a novel IL-17A

times, followed by RT-PCR analysis for TRAF4 and ΔNp63. Gene expression is graphed as mean fold induction over untreated ± SEM. (E) RT-PCR analysis of the indicated genes from nontumor or tumor samples of TRAF4<sup>+/-</sup> and TRAF4<sup>-/-</sup> mice at 22 wk of DMBA/TPA treatment. Gene expression is graphed as mean fold induction of tumor over nontumor ± SEM. (D and E) SEM was derived from three technical replicates. Data are representative of at least two independent experiments. (F and H) RT-PCR analysis of *Traf4*, *Steap4*, and ΔNp63 levels in ear tissue of mice who underwent treatment with PBS, IL-17A, and IL-17A + control siRNA, *Steap4* siRNA, or IL-17A ERK5 siRNA. Gene expression is graphed as mean fold induction of over PBS treatment ± SEM. SEM was derived from three technical replicates. (G and I) Immunohistochemistry staining of p63 on ear skin sections from WT mice intradermally injected with PBS, IL-17A, and IL-17A + control siRNA, *Steap4* siRNA1, or ERK5 siRNA as described in Figs. 5 I and 3 B. (B, G, and I) Bars, 50 μm. Data are representative of at least three independent experiments. Student's *t* test was used for all statistical analysis: \*, *P* < 0.05; \*\*, *P* < 0.01; \*\*\*, *P* < 0.001.

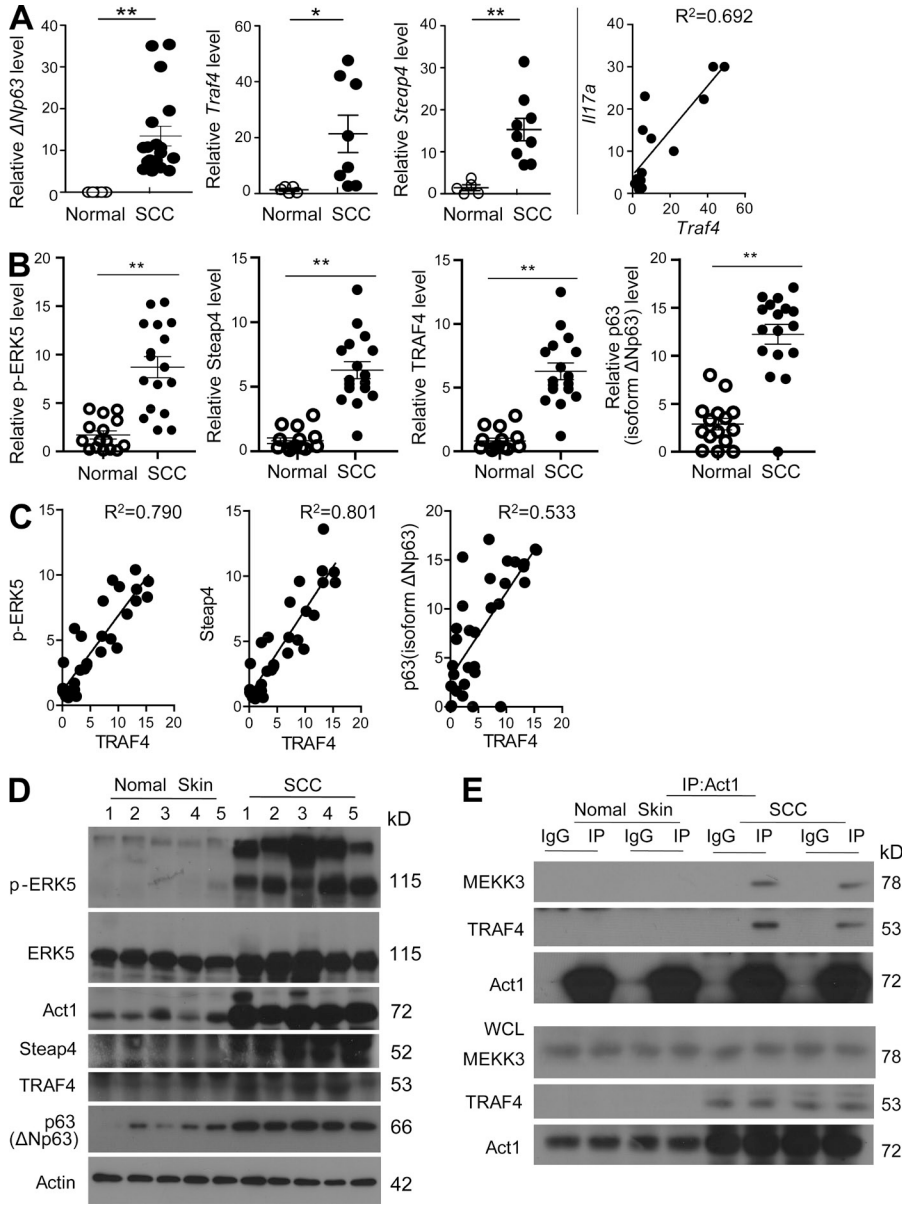


**Figure 7. The TRAF4-ERK5 is a dominant pathway in human skin SCC.** (A) RT-PCR analysis from FFPE sections of human normal or skin SCC samples. Gene expression is graphed as relative fold in SCC over normal skin. Each dot represents an independent sample. The last panel of A represents the linear regression of *Il17a* and *Traf4*. (B) Densitometric quantification of the indicated proteins in lysates of human normal skin ( $n = 15$ ) or SCC ( $n = 17$ ) as analyzed by Western blot. (A and B) Error bars represent SEM. SEM was derived from biological replicates. \*,  $P < 0.05$ ; \*\*,  $P < 0.01$  (Student's  $t$  test). (C) Linear regression of the indicated protein levels in human normal skin or SCC as detected by Western blot. (D) Representative results of Western blot analysis of normal human skin or SCC. Each lane represents samples from an individual patient. (E) Freshly collected normal human skin or SCC samples were lysed and subjected to immunoprecipitation with anti-Act1 antibody, followed by Western blot analysis. Each pair of lanes (IgG, IP) represents a sample from an individual patient. All the data are representative of three experiments.

signaling pathway via the IL-17R-Act1-TRAF4-MEKK3-ERK5 cascade that directly impacts keratinocyte proliferation and tumor formation. IL-17-induced Act1-TRAF4 interaction specifically directs the activation of the MEKK3-MEK5-ERK5 cascade, whereas it is dispensable for all the other IL-17-induced downstream signaling events including activation of ERK1/2, NF- $\kappa$ B, JNK, and p38. Although IL-17RC, Act1, TRAF4, MEKK3, or ERK5 deficiency resulted in a loss of IL-17-induced keratinocyte proliferation, keratinocyte-specific deletion of Act1 and deficiency of TRAF4 or IL-17RC was sufficient to protect mice from DMBA/TPA-induced carcinogenesis. We found that the dominance of this IL-17-TRAF4-ERK5 axis in the epidermis was established via a positive feedback on TRAF4 expression mediated by IL-17A-induced target genes *Steap4* and *p63*. Although knockdown of *Steap4* diminished IL-17-induced expansion of  $p63^+$

epidermal basal cells and ablated the positive feedback on TRAF4 expression, overexpression of *p63*, a transcription factor known to bind TRAF4 promoter, induced the expression of TRAF4 in keratinocytes. Collectively, our data suggest that the IL-17-induced *Steap4* might promote a positive feedback on TRAF4 expression via the expansion of  $p63^+$  cells, sustaining the IL-17-induced activation of the TRAF4-ERK5 axis for keratinocyte proliferation and tumor formation.

IL-17A and IL-17RA-deficient mice have been shown to be resistant to DMBA/TPA-induced carcinogenesis (Wang et al., 2010; He et al., 2012). Similarly, we found that IL-17RC $^{-/-}$  mice are more resistant to tumor formation compared with WT controls. The resistance to tumor formation was attributed to the role of IL-17A in sustaining a chronic inflammatory microenvironment that favors tumor formation. IL-17A was shown to induce inflammatory cytokines

like IL-6, which is a potent activator of the oncogenic STAT3, shown to be critical in tumor progression (Chan et al., 2004). We here report that keratinocyte-specific Act1 deletion was sufficient to protect mice from tumor formation. IL-6 expression as well as STAT3 activation was comparable in the TPA-treated epidermis or tumors from K5<sup>Cre</sup>Act1<sup>f/f</sup> mice compared with littermate controls. Instead, we show that IL-17A can directly induce keratinocyte proliferation through the activation of ERK5 for the induction of proliferation-associated genes. However, it is important to note that, in addition to reduction of ERK5 activation, IL-6 levels and STAT3 activation were reduced in tumors from IL-17RC and Act1 complete knockout mice but not in the K5<sup>Cre</sup>Act1<sup>f/f</sup> mice, suggesting IL-17 signaling in other cellular compartments (besides epidermis) might account for IL-6 production contributing to tumorigenesis (Fig. 1, I–O). IL-6 has been shown to partially contribute to colonic tumorigenesis (Wang et al., 2014). Because fibroblasts are highly responsive to IL-17 stimulation and have been shown to actively participate in tumorigenesis as part of the tumor microenvironment, future studies are required to investigate whether and how IL-17 signaling in fibroblasts (and other cellular compartments) contributes to skin tumorigenesis via production of protumorigenic inflammatory cytokines including IL-6.

Although little is known of the ERK5 pathway, direct evidence has shown that ERK5 can transcriptionally activate cyclin D as well as phosphorylate and stabilize c-myc (English et al., 1998; Mulloy et al., 2003). ERK5 reduction is associated with decreased tumor formation in colon cancer (Takaoka et al., 2012); hyperactive ERK5 has also been implicated in breast, lung, cervical, and prostate cancer (Castro and Lange, 2010; Yang et al., 2010). Here we show that Act1 coimmunoprecipitates with MEKK3, an upstream kinase of ERK5, and that this interaction was dependent on TRAF4. It is important to note that Act1 interacts with TRAF6 and TRAF2/5 to activate NF- $\kappa$ B and mediate posttranscriptional control, respectively. We have previously reported that TRAF4 competes with TRAF6 for the binding with Act1 in response to IL-17 stimulation (Zepp et al., 2012). We indeed found that TRAF4 deficiency specifically abolished IL-17-induced ERK5 activation, whereas IL-17-induced ERK1/2, NF- $\kappa$ B, JNK, and p38 activation and inflammatory genes (such as *IL-6* and *CXCL-1*) were slightly elevated in the absence of TRAF4. Therefore, the impact of the IL-17–TRAF4–ERK5 axis on keratinocyte proliferation and tumor formation is probably uncoupled from IL-17-induced inflammatory response. Future careful genetic studies are required to determine whether and how Act1–TRAF2/5- and Act1–TRAF6-mediated inflammatory cascades in the tumor microenvironment might contribute to skin tumorigenesis, including the production of IL-6 (Wang et al., 2010; He et al., 2012). It would also be important and interesting to investigate whether and how IL-6 and IL-17 might act cooperatively on tumor cells to promote tumor formation and progression.

Notably, TRAF4 is overexpressed in a wide-range of human malignancies and 70% of the tumors examined overexpressed

TRAF4 without alteration of the gene copy number. Interestingly, we found that *Traf4* expression was highly induced in the tumors from WT mice but not in the tumors from IL-17RC- and Act1-deficient mice. The elevated expression of TRAF4 might play a critical role in driving Act1 to favor the engagement of the MEKK3–ERK5 cascade, contributing to cell proliferation and tumorigenesis. We indeed found that *Traf4* was overexpressed in human skin SCC, in which we detected the expression of *Il17a*, the Act1–TRAF4–MEKK3 complex, and strong ERK5 activation, indicating this IL-17–TRAF4–ERK5 axis is hyperactivated in human SCC. One critical question was then how the dominance of this IL-17–TRAF4–ERK5 axis in the epidermis was established. Because *Traf4* was highly expressed in mouse skin tumors in an IL-17R- and Act1-dependent manner, we hypothesized that the IL-17–TRAF4–ERK5 axis might have a positive feedback on TRAF4 expression. A previous study reported that transcription factor p63 binds to the TRAF4 promoter and induces transcription from the TRAF4 promoter (Gu et al., 2007). Notably, although p63 plays an essential role in maintenance of the proliferative potential of epidermal stem cells (Yi et al., 2008), p63 expression is detected in basal cells and SCCs, as well as in transitional cell carcinomas. Although overexpression of *p63* induced the expression of *Traf4* in keratinocytes, both *p63* and *Traf4* expression were induced by IL-17 stimulation. Furthermore, we found that p63 was also highly expressed in mouse skin tumors in an IL-17R- and Act1-dependent manner and overexpressed in human SCCs, correlating with the expression of TRAF4 in the tumors. Collectively, we propose that *p63*-mediated TRAF4 overexpression might be an important feature of tumor cells, in which an elevated TRAF4 expression allows IL-17 to activate the IL-17R–Act1–TRAF4–MEKK3–ERK5 axis as the dominant pathway to promote tumorigenesis.

We further identified *Steap4*, a metalloendopeptidase, as a critical link for the positive feedback loop of the IL-17–TRAF4–ERK5 pathway. We found that IL-17A stimulation resulted in strong up-regulation of *Steap4* in cultured keratinocytes. IL-17A-induced *Steap4* expression was abolished in Act1-deficient cells and substantially reduced in MEKK3-, TRAF4-, and ERK5-deficient keratinocytes. *Steap4* is a metalloprotease that has been shown to be involved in prostate cancer, metabolism, and inflammation (Korkmaz et al., 2005; Wellen et al., 2007; Gomes et al., 2012; ten Freyhaus et al., 2012; Gauss et al., 2013). We indeed found that knockdown of *Steap4* diminished IL-17-induced expansion of the p63<sup>+</sup> basal cells in the epidermis, implicating the critical role of *Steap4* in maintaining the survival/proliferation of these progenitor cells. Consistent with the role of p63 in driving TRAF4 expression, *Steap4* knockdown also blocked IL-17-induced positive feedback on TRAF4 expression with greatly reduced ERK5 activation, indicating this IL-17–TRAF4–ERK5 positive circuit might take place in the p63<sup>+</sup> basal cells. In support of this, we found that *Steap4* was highly expressed in mouse skin tumors in an IL-17R- Act1- and TRAF4-dependent manner and overexpressed in human SCCs, correlating with the

expression of TRAF4 and p63 in the tumors. One remaining question is how IL-17–induced ERK5 activation leads to up-regulation of *Steap4*. Although C/EBP $\alpha$  has been implicated in regulation of *Steap4* gene transcription (Ramadoss et al., 2010), we found that IL-17–induced ERK5 activation leads to induction of C/EBP transcription activity (unpublished data), suggesting that activation of ERK5 might induce the expression of *Steap4* via activation of the C/EBP transcription family.

Although *Steap4* is known as a cell surface metalloredoxase, *Steap4* retains activity at acidic pH, suggesting it may also function within intracellular organelles (Gauss et al., 2013). Importantly, flavin-dependent NOX activity was observed for *Steap4*, implicating its role in NADPH homeostasis (Gauss et al., 2013). Interestingly, NOX was shown to play a critical role in promoting glycolysis in cancer cells by generating NAD<sup>+</sup>, a substrate for one of the key glycolytic reactions. Inhibition of NOX attenuates cancer cell proliferation and tumor growth (Lu et al., 2012). Considering the NOX activity of *Steap4*, it is possible that overexpression of *Steap4* may directly alter cellular metabolism in tumor cells, where proliferating cells may need an increased expression of *Steap4* to meet the increased demands for nutrients. Though the role of STEAP4 in the epidermis is currently unclear, our findings indicate that this IL-17A–induced gene may play a role in keratinocytes and potentially affect the metabolism and survival of epidermal basal cells. Although IL-17–dependent ERK5 activation induced c-myc expression that is known to promote cell cycle progression, IL-17–induced *Steap4* may provide the necessary metabolic state of the basal cells for the IL-17–induced proliferative response in the epidermis. Notably, *Steap4* is elevated in human skin SCCs. Future studies are required to determine whether the elevated *Steap4* expression may affect the glycolytic pathway and survival of proliferating and tumor cells, which may provide a new cancer therapy.

## MATERIALS AND METHODS

**Animals.** 6–8-wk-old mice were used for all experiments. All experiments were conducted in accordance with Institutional Animal Care and Use Committee guidelines at the Cleveland Clinic Lerner Research Institute. To generate K5<sup>Cre</sup>Act1<sup>f/f</sup> mice, K5<sup>Cre</sup> mice were bred to Act1 flox mice. K5<sup>Cre</sup> mice were provided by T. Egelhoff (Cleveland Clinic Lerner Research Institute, Cleveland, OH). WT C57BL/6 mice were purchased from the Jackson Laboratory. All experiments used sex- and age-matched littermates. TRAF4<sup>-/-</sup> mice on a C57BL/6 background were generated as described previously (Shiels et al., 2000). Act1<sup>-/-</sup> mice and Act1<sup>f/f</sup> mice were as described previously (Qian et al., 2004). IL-17RC<sup>-/-</sup> mice were as described previously (Zheng et al., 2008). MEKK3<sup>f/f</sup> mice were as described previously (Wang et al., 2009). ERK5<sup>f/f</sup> keratinocytes were isolated from skin tissue provided by C. Tourmier and C.M. Vines. The background of ERK5<sup>f/f</sup> mice was as described previously (Finegan et al., 2009). Act1<sup>-/-</sup> mice used in the DMBA/TPA model were on a BALB/c background. Act1<sup>-/-</sup> mice for all other experiments were crossed back to C57BL/6 mice for at least 10 generations.

**Two-stage DMBA/TPA tumorigenesis.** 6-wk-old gender-matched mice were used for two-stage tumorigenesis. Tumorigenesis was initiated with one topical application of 100  $\mu$ M DMBA (Sigma-Aldrich) in 200  $\mu$ l acetone to the shaved dorsal skin of each mouse. 2 wk after initiation, mice were treated topically with 30  $\mu$ g TPA (Sigma-Aldrich) in 200  $\mu$ l acetone

twice a week for 23 wk. Tumor incidence and numbers were monitored weekly. Tumors >1 mm were counted and recorded.

**TPA-induced skin proliferation.** 12.5  $\mu$ g TPA in 200  $\mu$ l acetone was applied to the shaved dorsal skin of 6–8-wk-old mice on days 0 and 4. Skin samples were collected at day 6. For BrdU incorporation, 100  $\mu$ g BrdU (BD) in 500  $\mu$ l PBS was injected intraperitoneally 24 h before sample collection.

**IL-17–induced skin proliferation, in vivo knockdown, and inhibitor injection.** 20  $\mu$ l IL-17A (500 ng/20  $\mu$ l PBS; R&D Systems) was injected intradermally daily for 6 d in the right ear of 6–8-wk-old mice. As a control, 20  $\mu$ l PBS was injected into the left ear of each mouse. On day 7, treated ear tissues were collected for histology and RNA analysis. For BrdU incorporation, 100  $\mu$ g BrdU (BD) in 500  $\mu$ l PBS was injected intraperitoneally 24 h before sample collection. For siRNA in vivo injection, the target sequences for ERK5 and *Steap4* knockdown (ERK5 siRNA and *Steap4* siRNA1) were described in previous studies (Woo et al., 2006; Wellen et al., 2007). The *Steap4* siRNA2 target sequence was 5'–CCCUCGCGCUUAUUAUUUUUG–3'. The control siRNA sequence was 5'–UGGUUUACAUGUCGACUAA–3'. siRNA was synthesized by GE Healthcare. siRNA was dissolved in PBS. PBS or IL-17A was injected daily for 6 d while siRNA was administered by intradermal injection (5 nmol each injection) at days 0, 1, and 4, together with IL-17A. For the MEK5 inhibitor injection experiment, mice were injected with PBS, Bix 02189 (dissolved in DMSO and added to PBS to a 5  $\mu$ M final concentration) alone, 500 ng IL-17A plus DMSO, or 500 ng IL-17A plus MEK5i (Bix 02189, 5  $\mu$ M) daily for 6 d.

**Cell culture and reagents.** Primary keratinocytes were cultured in keratinocyte serum-free media (K-SFM) with supplement purchased from Life Technologies with 100  $\mu$ g/ml penicillin G and 100  $\mu$ g/ml streptomycin. Media was changed every 2 d. Kidney epithelial cells were maintained in DMEM supplemented with 10% (volume/volume) FBS (Hyclone), 100  $\mu$ g/ml penicillin G, and 100  $\mu$ g/ml streptomycin. Recombinant IL-17A, IL-17F, and TNF were from R&D Systems; anti-Flag (M2) and anti-human STEAP4 antibody were from Sigma-Aldrich; antibody to phosphorylated Jnk, antibody to phosphorylated I $\kappa$ B $\alpha$ , phosphorylated p-38, phosphorylated ERK5, ERK5, phosphorylated STAT3, STAT3, ERK1/2, phosphorylated 4EBP, phosphorylated S6, and anti-p63 for Western blotting were from Cell Signaling Technology; antibody to phosphorylated ERK, actin, anti-BrdU, and anti-p63 for staining were from Santa Cruz Biotechnology, Inc. MEK5 inhibitor (MEK5i, Bix 02189) was ordered from Selleck. IL-6 neutralizing antibody was purchased from BD.

**Primary keratinocyte isolation, proliferation, and adenovirus infection.** Keratinocytes were isolated from the skin from newborn pups (days 1–2). Skins were floated dermis side down on 0.25% trypsin (without EDTA) overnight at 4°C. The next day, the epidermis was separated from the dermis, minced, and filtered with a 40- $\mu$ m strainer. For keratinocyte proliferation assay, isolated cells at a density of  $0.2 \times 10^6$  cells/ml were cultured in 12-well plates (triple replicated) in K-SFM (Life Technologies) with supplement (Life Technologies). The next day (day 0) as the keratinocytes attached, fresh media was used and 100 ng/ml IL-17A or 2  $\mu$ g/ml IL-17A + anti-IL-6 neutralizing antibody was added into the media for a 5-d culture. Cells were detached into single cell suspension with trypsin and counted at the indicated days. For adenovirus infection, keratinocytes were cultured at a density of  $0.79 \times 10^6$  cells/ml in K-SFM with supplement. Adenovirus expressing Cre recombinase was purchased from Vector Laboratories. Cells were infected with 1:10,000 dilution of the viruses for 2 d.

**Immunohistochemistry staining.** Tissues were fixed with 10% formalin and processed into paraffin tissue blocks according to routine methods by AML Laboratories or were embedded in optimum cutting temperature compound and were sectioned or serially sectioned to obtain consecutive levels. Skin tissue was processed by AML Laboratories. Paraffin-embedded sections were used for hematoxylin and eosin (H&E), BrdU (Santa Cruz

Biotechnology, Inc.), Krt10 (EMD Millipore), and p63 (Santa Cruz Biotechnology, Inc.) staining. Paraffin-embedded sections were antigen retrieved with sodium citrate. Frozen sections in OCT were used for anti-CD4 (BD), Gr1 (BD), and Ki67 (Dako). All images were captured with a DP71 digital camera (Olympus) attached to a BX41 microscope (Olympus).

**BrdU staining of keratinocytes.** Cultured primary keratinocytes were washed once with PBS and changed to K-SFM without supplement along with 100 ng/ml IL-17A treatment for 24 h. 10  $\mu$ M BrdU was added during the last 2 h of stimulation. Cells were then fixed for 20 min at room temperature with 2% paraformaldehyde and washed twice with PBS, followed by incubation with 2N HCL at 37°C for 30 min. The reaction was stopped with boric acid followed by three washes with PBS.

**Western blotting and immunoprecipitation.** Keratinocytes were starved overnight by incubating cells in SFM without supplement, followed by 100 ng/ml IL-17A stimulation for the indicated times. Immunoprecipitation was performed as described previously (Wang et al., 2013).

**RNA isolation and RT-PCR.** Skin samples were collected, placed directly in TRIzol, and frozen over dry ice. For RNA isolation, samples were thawed, minced with scissors, and homogenized using an OMNI TH tissue homogenizer (Omni International). Homogenized samples were centrifuged at 13,000 rpm for 10 min, and the supernatant was used for RNA isolation from TRIzol (Invitrogen) according to the manufacturer's instructions. 1  $\mu$ g RNA from TPA-treated skin samples was used to synthesize cDNA using Superscript II. Gene expression analysis was determined using SYBR Green master mix. Keratinocyte RNA was isolated using TRIzol according to the manufacturer's instructions, followed by DNase treatment (QIAGEN) and RNA cleanup using the RNA MinElute kit (QIAGEN). 200 ng RNA was used to synthesize cDNA. For RNA from formalin-fixed paraffin-embedded (FFPE) samples, normal and skin SCC tissues for RNA extraction were derived from FFPE human skin biopsies from several individuals under a research protocol approved by the Cleveland Clinic Foundation Institutional Review Board. One 30- $\mu$ m section of each sample was used for RNA isolation using the RNeasy FFPE kit (QIAGEN). Samples in 1.5-ml microcentrifuge tubes were deparaffinized using 1 ml xylenes by vortexing, followed by three washes with 100% ethanol to remove the xylenes. RNA was extracted according to the manufacturer's protocol (QIAGEN). CYBR Green PCR Master Mix (Applied Biosystems) was used for RT-PCR. Primer sequences for RT-PCR are listed in Table S1.

**Human specimen collection.** Normal skin specimens were collected from patients undergoing cosmetic surgical procedures, whereas SCC specimens were collected from patients undergoing surgery to remove skin tumors that were diagnosed as SCCs by a dermatopathologist. All these samples were from the Cleveland Clinic Main Hospital (Table S2). Sample collection and processing were on a protocol titled "Molecular Signaling and Gene Expression in Ultraviolet (UV) Light-Induced Skin Cancers," approved by the Institutional Review Board of the Cleveland Clinic Foundation.

**Online supplemental material.** Table S1 shows the primers used for RT-PCR. Table S2 shows specimen information of human skin SCCs. Online supplemental material is available at <http://www.jem.org/cgi/content/full/jem.20150204/DC1>.

We thank T. Egelhoff for kindly providing us with the K5<sup>Cre</sup> mice; AML Laboratories and the Lerner Research Institute Histology Core for processing tissue samples for histology; J. Ma and W. Qian for technical support; E. Hamburg and the Atit Lab (College of Arts and Science, Case Western Reserve University) for immunohistochemistry technical support; and Drs. C. Poblete-Lopez, J. Lucas, and J. Meine (Department of Dermatology, Cleveland Clinic) for the help of specimen collection.

This work is supported by the US National Institutes of Health (grants P01CA062220-16A1, 1R01NS071996, and 1P01 HL103453 to X. Li; and T32 GM007250 to the Case Western Reserve University Medical Scientist Training

Program and T32 AI 89474-1 to the Case Western Reserve University Immunology Training Program, for support of L. Wu).

W. Ouyang is an employee of Genentech. The authors declare no additional competing financial interests.

Submitted: 2 February 2015

Accepted: 7 August 2015

## REFERENCES

- Bulek, K., C. Liu, S. Swaidani, L. Wang, R.C. Page, M.F. Gulen, T. Herjan, A. Abbadi, W. Qian, D. Sun, et al. 2011. The inducible kinase IKKi is required for IL-17-dependent signaling associated with neutrophilia and pulmonary inflammation. *Nat. Immunol.* 12:844–852. <http://dx.doi.org/10.1038/ni.2080>
- Camilleri-Broët, S., I. Cremer, B. Marmey, E. Comperat, F.Viguié, J. Audouin, M.C. Rio, W.H. Fridman, C. Sautès-Fridman, and C.H. Régnier. 2007. TRAF4 overexpression is a common characteristic of human carcinomas. *Oncogene*. 26:142–147. <http://dx.doi.org/10.1038/sj.onc.1209762>
- Castro, N.E., and C.A. Lange. 2010. Breast tumor kinase and extracellular signal-regulated kinase 5 mediate Met receptor signaling to cell migration in breast cancer cells. *Breast Cancer Res.* 12:R60. <http://dx.doi.org/10.1186/bcr2622>
- Chae, W.J., T.F. Gibson, D. Zelterman, L. Hao, O. Henegariu, and A.L. Bothwell. 2010. Ablation of IL-17A abrogates progression of spontaneous intestinal tumorigenesis. *Proc. Natl. Acad. Sci. USA.* 107:5540–5544. <http://dx.doi.org/10.1073/pnas.0912675107>
- Chan, K.S., S. Sano, K. Kiguchi, J. Anders, N. Komazawa, J. Takeda, and J. DiGiovanni. 2004. Disruption of Stat3 reveals a critical role in both the initiation and the promotion stages of epithelial carcinogenesis. *J. Clin. Invest.* 114:720–728. <http://dx.doi.org/10.1172/JCI200421032>
- Chang, S.H., H. Park, and C. Dong. 2006. Act1 adaptor protein is an immediate and essential signaling component of interleukin-17 receptor. *J. Biol. Chem.* 281:35603–35607. <http://dx.doi.org/10.1074/jbc.C600256200>
- Chung, A.S., X. Wu, G. Zhuang, H. Ngu, I. Kasman, J. Zhang, J.M. Vernes, Z. Jiang, Y.G. Meng, F.V. Peale, et al. 2013. An interleukin-17-mediated paracrine network promotes tumor resistance to anti-angiogenic therapy. *Nat. Med.* 19:1114–1123. <http://dx.doi.org/10.1038/nm.3291>
- Coussens, L.M., and Z. Werb. 2002. Inflammation and cancer. *Nature*. 420:860–867. <http://dx.doi.org/10.1038/nature01322>
- Crish, J., M.A. Conti, T. Sakai, R.S. Adelman, and T.T. Egelhoff. 2013. Keratin 5-Cre-driven excision of nonmuscle myosin IIA in early embryo trophectoderm leads to placenta defects and embryonic lethality. *Dev. Biol.* 382:136–148. <http://dx.doi.org/10.1016/j.ydbio.2013.07.017>
- Deschênes-Simard, X., F. Kottakis, S. Meloche, and G. Ferbeyre. 2014. ERKs in cancer: friends or foes? *Cancer Res.* 74:412–419. <http://dx.doi.org/10.1158/0008-5472.CAN-13-2381>
- DeYoung, M.P., and L.W. Ellisen. 2007. p63 and p73 in human cancer: defining the network. *Oncogene*. 26:5169–5183. <http://dx.doi.org/10.1038/sj.onc.1210337>
- Drew, B.A., M.E. Burrow, and B.S. Beckman. 2012. MEK5/ERK5 pathway: the first fifteen years. *Biochim. Biophys. Acta.* 1825:37–48. <http://dx.doi.org/10.1016/j.bbcan.2011.10.002>
- English, J.M., G. Pearson, R. Baer, and M.H. Cobb. 1998. Identification of substrates and regulators of the mitogen-activated protein kinase ERK5 using chimeric protein kinases. *J. Biol. Chem.* 273:3854–3860. <http://dx.doi.org/10.1074/jbc.273.7.3854>
- Finegan, K.G., X. Wang, E.J. Lee, A.C. Robinson, and C. Tournier. 2009. Regulation of neuronal survival by the extracellular signal-regulated protein kinase 5. *Cell Death Differ.* 16:674–683. <http://dx.doi.org/10.1038/cdd.2008.193>
- Finegan, K.G., D. Perez-Madrigal, J.R. Hitchin, C.C. Davies, A.M. Jordan, and C. Tournier. 2015. ERK5 is a critical mediator of inflammation-driven cancer. *Cancer Res.* 75:742–753. <http://dx.doi.org/10.1158/0008-5472.CAN-13-3043>
- Gaffen, S.L. 2009. Structure and signalling in the IL-17 receptor family. *Nat. Rev. Immunol.* 9:556–567. <http://dx.doi.org/10.1038/nri2586>
- Gauss, G.H., M.D. Kleven, A.K. Sendamarai, M.D. Fleming, and C.M. Lawrence. 2013. The crystal structure of six-transmembrane epithelial

- antigen of the prostate 4 (Steap4), a ferri/cuprireductase, suggests a novel interdomain flavin-binding site. *J. Biol. Chem.* 288:20668–20682. <http://dx.doi.org/10.1074/jbc.M113.479154>
- Golden, J.B., T.S. McCormick, and N.L. Ward. 2013. IL-17 in psoriasis: implications for therapy and cardiovascular co-morbidities. *Cytokine*. 62:195–201. <http://dx.doi.org/10.1016/j.cyto.2013.03.013>
- Gomes, I.M., C.J. Maia, and C.R. Santos. 2012. STEAP proteins: from structure to applications in cancer therapy. *Mol. Cancer Res.* 10:573–587. <http://dx.doi.org/10.1158/1541-7786.MCR-11-0281>
- Grivennikov, S.I., K. Wang, D. Mucida, C.A. Stewart, B. Schnabl, D. Jauch, K. Taniguchi, G.Y. Yu, C.H. Osterreicher, K.E. Hung, et al. 2012. Adenoma-linked barrier defects and microbial products drive IL-23/IL-17-mediated tumour growth. *Nature*. 491:254–258. <http://dx.doi.org/10.1038/nature11465>
- Gu, X., P.J. Coates, S.F. MacCallum, L. Boldrup, B. Sjöström, and K. Nylander. 2007. TRAF4 is potently induced by TAP63 isoforms and localised according to differentiation in SCCHN. *Cancer Biol. Ther.* 6:1986–1990. <http://dx.doi.org/10.4161/cbt.6.12.5002>
- Hartupee, J., C. Liu, M. Novotny, D. Sun, X. Li, and T.A. Hamilton. 2009. IL-17 signaling for mRNA stabilization does not require TNF receptor-associated factor 6. *J. Immunol.* 182:1660–1666. <http://dx.doi.org/10.4049/jimmunol.182.3.1660>
- He, D., H. Li, N. Yusuf, C.A. Elmets, M. Athar, S.K. Katiyar, and H. Xu. 2012. IL-17 mediated inflammation promotes tumor growth and progression in the skin. *PLoS ONE*. 7:e32126. <http://dx.doi.org/10.1371/journal.pone.0032126>
- Hyun, Y.S., D.S. Han, A.R. Lee, C.S. Eun, J. Youn, and H.Y. Kim. 2012. Role of IL-17A in the development of colitis-associated cancer. *Carcinogenesis*. 33:931–936. <http://dx.doi.org/10.1093/carcin/bgs106>
- Ihrig, R.A., M.R. Marques, B.T. Nguyen, J.S. Horner, C. Papazoglu, R.T. Bronson, A.A. Mills, and L.D. Attardi. 2005. Perp is a p63-regulated gene essential for epithelial integrity. *Cell*. 120:843–856. <http://dx.doi.org/10.1016/j.cell.2005.01.008>
- Iwakura, Y., S. Nakae, S. Saijo, and H. Ishigame. 2008. The roles of IL-17A in inflammatory immune responses and host defense against pathogens. *Immunol. Rev.* 226:57–79. <http://dx.doi.org/10.1111/j.1600-065X.2008.00699.x>
- Korkmaz, C.G., K.S. Korkmaz, P. Kurys, C. Elbi, L. Wang, T.I. Klock, C. Hammarstrom, G. Troen, A. Svindland, G.L. Hager, and F. Saatcioglu. 2005. Molecular cloning and characterization of STAMP2, an androgen-regulated six transmembrane protein that is overexpressed in prostate cancer. *Oncogene*. 24:4934–4945. <http://dx.doi.org/10.1038/sj.onc.1208677>
- Langowski, J.L., X. Zhang, L. Wu, J.D. Mattson, T. Chen, K. Smith, B. Basham, T. McClanahan, R.A. Kastelein, and M. Oft. 2006. IL-23 promotes tumour incidence and growth. *Nature*. 442:461–465. <http://dx.doi.org/10.1038/nature04808>
- Liu, J., Y. Duan, X. Cheng, X. Chen, W. Xie, H. Long, Z. Lin, and B. Zhu. 2011. IL-17 is associated with poor prognosis and promotes angiogenesis via stimulating VEGF production of cancer cells in colorectal carcinoma. *Biochem. Biophys. Res. Commun.* 407:348–354. <http://dx.doi.org/10.1016/j.bbrc.2011.03.021>
- Lu, W., Y. Hu, G. Chen, Z. Chen, H. Zhang, F. Wang, L. Feng, H. Pelicano, H. Wang, M.J. Keating, et al. 2012. Novel role of NOX in supporting aerobic glycolysis in cancer cells with mitochondrial dysfunction and as a potential target for cancer therapy. *PLoS Biol.* 10:e1001326. <http://dx.doi.org/10.1371/journal.pbio.1001326>
- Mauro, C., P. Vito, S. Mellone, F. Pacifico, A. Chariot, S. Formisano, and A. Leonardi. 2003. Role of the adaptor protein CIKS in the activation of the IKK complex. *Biochem. Biophys. Res. Commun.* 309:84–90. [http://dx.doi.org/10.1016/S0006-291X\(03\)01532-8](http://dx.doi.org/10.1016/S0006-291X(03)01532-8)
- Mulloy, R., S. Salinas, A. Philips, and R.A. Hipskind. 2003. Activation of cyclin D1 expression by the ERK5 cascade. *Oncogene*. 22:5387–5398. <http://dx.doi.org/10.1038/sj.onc.1206839>
- Nithianandarajah-Jones, G.N., B. Wilm, C.E. Goldring, J. Müller, and M.J. Cross. 2012. ERK5: structure, regulation and function. *Cell. Signal.* 24:2187–2196. <http://dx.doi.org/10.1016/j.cellsig.2012.07.007>
- Nogral, K.E., L.C. Zaba, E. Guttman-Yassky, J. Fuentes-Duculan, M. Suárez-Fariñas, I. Cardinale, A. Khatcherian, J. Gonzalez, K.C. Pierson, T.R. White, et al. 2008. Th17 cytokines interleukin (IL)-17 and IL-22 modulate distinct inflammatory and keratinocyte-response pathways. *Br. J. Dermatol.* 159:1092–1102. <http://dx.doi.org/10.1111/j.1365-2133.2008.08769.x>
- Numasaki, M., J. Fukushi, M. Ono, S.K. Narula, P.J. Zavadny, T. Kudo, P.D. Robbins, H. Tahara, and M.T. Lotze. 2003. Interleukin-17 promotes angiogenesis and tumor growth. *Blood*. 101:2620–2627. <http://dx.doi.org/10.1182/blood-2002-05-1461>
- Puel, A., S. Cypowj, J. Bustamante, J.F. Wright, L. Liu, H.K. Lim, M. Migaud, L. Israel, M. Chrabieh, M. Audry, et al. 2011. Chronic mucocutaneous candidiasis in humans with inborn errors of interleukin-17 immunity. *Science*. 332:65–68. <http://dx.doi.org/10.1126/science.1200439>
- Qian, Y., J. Qin, G. Cui, M. Naramura, E.C. Snow, C.F. Ware, R.L. Fairchild, S.A. Omori, R.C. Rickert, M. Scott, et al. 2004. Act1, a negative regulator in CD40- and BAFF-mediated B cell survival. *Immunity*. 21:575–587. <http://dx.doi.org/10.1016/j.immuni.2004.09.001>
- Qian, Y., C. Liu, J. Hartupee, C.Z. Altuntas, M.F. Gulen, D. Jane-Wit, J. Xiao, Y. Lu, N. Giltaiy, J. Liu, et al. 2007. The adaptor Act1 is required for interleukin 17-dependent signaling associated with autoimmune and inflammatory disease. *Nat. Immunol.* 8:247–256. <http://dx.doi.org/10.1038/ni1439>
- Ramados, P., F. Chiappini, M. Bilban, and A.N. Hollenberg. 2010. Regulation of hepatic six transmembrane epithelial antigen of prostate 4 (STEAP4) expression by STAT3 and CCAAT/enhancer-binding protein alpha. *J. Biol. Chem.* 285:16453–16466. <http://dx.doi.org/10.1074/jbc.M109.066936>
- Riedemann, N.C., T.A. Neff, R.F. Guo, K.D. Bernacki, I.J. Laudes, J.V. Sarma, J.D. Lambris, and P.A. Ward. 2003. Protective effects of IL-6 blockade in sepsis are linked to reduced C5a receptor expression. *J. Immunol.* 170:503–507. <http://dx.doi.org/10.4049/jimmunol.170.1.503>
- Rocco, J.W., C.O. Leong, N. Kuperwasser, M.P. DeYoung, and L.W. Ellisen. 2006. p63 mediates survival in squamous cell carcinoma by suppression of p73-dependent apoptosis. *Cancer Cell*. 9:45–56. <http://dx.doi.org/10.1016/j.ccr.2005.12.013>
- Rochman, I., W.E. Paul, and S.Z. Ben-Sasson. 2005. IL-6 increases primed cell expansion and survival. *J. Immunol.* 174:4761–4767. <http://dx.doi.org/10.4049/jimmunol.174.8.4761>
- Shiels, H., X. Li, P.T. Schumacker, E. Maltepe, P.A. Padrid, A. Sperling, C.B. Thompson, and T. Lindsten. 2000. TRAF4 deficiency leads to tracheal malformation with resulting alterations in air flow to the lungs. *Am. J. Pathol.* 157:679–688. [http://dx.doi.org/10.1016/S0002-9440\(10\)64578-6](http://dx.doi.org/10.1016/S0002-9440(10)64578-6)
- Sun, D., M. Novotny, K. Bulek, C. Liu, X. Li, and T. Hamilton. 2011. Treatment with IL-17 prolongs the half-life of chemokine CXCL1 mRNA via the adaptor TRAF5 and the splicing-regulatory factor SF2 (ASF). *Nat. Immunol.* 12:853–860. <http://dx.doi.org/10.1038/ni.2081>
- Takaoka, Y., Y. Shimizu, H. Hasegawa, Y. Ouchi, S. Qiao, M. Nagahara, M. Ichihara, J.D. Lee, K. Adachi, M. Hamaguchi, and T. Iwamoto. 2012. Forced expression of miR-143 represses ERK5/c-Myc and p68/p72 signaling in concert with miR-145 in gut tumors of *Ape<sup>Min</sup>* mice. *PLoS ONE*. 7:e42137. <http://dx.doi.org/10.1371/journal.pone.0042137>
- Tatake, R.J., M.M. O'Neill, C.A. Kennedy, A.L. Wayne, S. Jakes, D. Wu, S.Z. Kugler Jr., M.A. Kashem, P. Kaplita, and R.J. Snow. 2008. Identification of pharmacological inhibitors of the MEK5/ERK5 pathway. *Biochem. Biophys. Res. Commun.* 377:120–125. <http://dx.doi.org/10.1016/j.bbrc.2008.09.087>
- ten Freyhaus, H., E.S. Calay, A. Yalcin, S.N. Vallerie, L. Yang, Z.Z. Calay, F. Saatcioglu, and G.S. Hotamisligil. 2012. Stamp2 controls macrophage inflammation through nicotinamide adenine dinucleotide phosphate homeostasis and protects against atherosclerosis. *Cell Metab.* 16:81–89. <http://dx.doi.org/10.1016/j.cmet.2012.05.009>
- Tong, Z., X.O. Yang, H. Yan, W. Liu, X. Niu, Y. Shi, W. Fang, B. Xiong, Y. Wan, and C. Dong. 2012. A protective role by interleukin-17F in colon tumorigenesis. *PLoS ONE*. 7:e34959. <http://dx.doi.org/10.1371/journal.pone.0034959>
- Toy, D., D. Kugler, M. Wolfson, T. Vanden Bos, J. Gurgel, J. Derry, J. Tocker, and J. Peschon. 2006. Cutting edge: interleukin 17 signals through a heteromeric receptor complex. *J. Immunol.* 177:36–39. <http://dx.doi.org/10.4049/jimmunol.177.1.36>
- Wang, C., L. Wu, K. Bulek, B.N. Martin, J.A. Zepp, Z. Kang, C. Liu, T. Herjan, S. Misra, J.A. Carman, et al. 2013. The psoriasis-associated D10N variant

- of the adaptor Act1 with impaired regulation by the molecular chaperone hsp90. *Nat. Immunol.* 14:72–81. <http://dx.doi.org/10.1038/ni.2479>
- Wang, K., M.K. Kim, G. Di Caro, J. Wong, S. Shalapour, J. Wan, W. Zhang, Z. Zhong, E. Sanchez-Lopez, L.W. Wu, et al. 2014. Interleukin-17 receptor a signaling in transformed enterocytes promotes early colorectal tumorigenesis. *Immunity*. 41:1052–1063. <http://dx.doi.org/10.1016/j.immuni.2014.11.009>
- Wang, L., T. Yi, W. Zhang, D.M. Pardoll, and H. Yu. 2010. IL-17 enhances tumor development in carcinogen-induced skin cancer. *Cancer Res.* 70:10112–10120. <http://dx.doi.org/10.1158/0008-5472.CAN-10-0775>
- Wang, X., X. Chang, V. Facchinetti, Y. Zhuang, and B. Su. 2009. MEKK3 is essential for lymphopenia-induced T cell proliferation and survival. *J. Immunol.* 182:3597–3608. <http://dx.doi.org/10.4049/jimmunol.0803738>
- Wellen, K.E., R. Fucho, M.F. Gregor, M. Furuhashi, C. Morgan, T. Lindstad, E. Vaillancourt, C.Z. Gorgun, F. Saatcioglu, and G.S. Hotamisligil. 2007. Coordinated regulation of nutrient and inflammatory responses by STAMP2 is essential for metabolic homeostasis. *Cell*. 129:537–548. <http://dx.doi.org/10.1016/j.cell.2007.02.049>
- Wilke, C.M., I. Kryczek, S. Wei, E. Zhao, K. Wu, G. Wang, and W. Zou. 2011. Th17 cells in cancer: help or hindrance? *Carcinogenesis*. 32:643–649. <http://dx.doi.org/10.1093/carcin/bgr019>
- Wong, C.E., J.S. Yu, D.A. Quigley, M.D. To, K.Y. Jen, P.Y. Huang, R. Del Rosario, and A. Balmain. 2013. Inflammation and Hras signaling control epithelial-mesenchymal transition during skin tumor progression. *Genes Dev.* 27:670–682. <http://dx.doi.org/10.1101/gad.210427.112>
- Woo, C.H., M.P. Massett, T. Shishido, S. Itoh, B. Ding, C. McClain, W. Che, S.R. Vulapalli, C. Yan, and J. Abe. 2006. ERK5 activation inhibits inflammatory responses via peroxisome proliferator-activated receptor delta (PPAR $\delta$ ) stimulation. *J. Biol. Chem.* 281:32164–32174. <http://dx.doi.org/10.1074/jbc.M602369200>
- Yang, Q., X. Deng, B. Lu, M. Cameron, C. Fearn, M.P. Patricelli, J.R. Yates III, N.S. Gray, and J.D. Lee. 2010. Pharmacological inhibition of BMK1 suppresses tumor growth through promyelocytic leukemia protein. *Cancer Cell*. 18:258–267. <http://dx.doi.org/10.1016/j.ccr.2010.08.008>
- Yen, D., J. Cheung, H. Scheerens, F. Poulet, T. McClanahan, B. McKenzie, M.A. Kleinschek, A. Owyang, J. Mattson, W. Blumenschein, et al. 2006. IL-23 is essential for T cell-mediated colitis and promotes inflammation via IL-17 and IL-6. *J. Clin. Invest.* 116:1310–1316. <http://dx.doi.org/10.1172/JCI21404>
- Yi, R., M.N. Poy, M. Stoffel, and E. Fuchs. 2008. A skin microRNA promotes differentiation by repressing ‘stemness’. *Nature*. 452:225–229. <http://dx.doi.org/10.1038/nature06642>
- Zepp, J.A., C. Liu, W. Qian, L. Wu, M.F. Gulen, Z. Kang, and X. Li. 2012. Cutting edge: TNF receptor-associated factor 4 restricts IL-17-mediated pathology and signaling processes. *J. Immunol.* 189:33–37. <http://dx.doi.org/10.4049/jimmunol.1200470>
- Zhang, B., C. Liu, W. Qian, Y. Han, X. Li, and J. Deng. 2014. Structure of the unique SEFIR domain from human interleukin 17 receptor A reveals a composite ligand-binding site containing a conserved  $\alpha$ -helix for Act1 binding and IL-17 signaling. *Acta Crystallogr. D Biol. Crystallogr.* 70:1476–1483. <http://dx.doi.org/10.1107/S1399004714005227>
- Zhang, J.P., J. Yan, J. Xu, X.H. Pang, M.S. Chen, L. Li, C. Wu, S.P. Li, and L. Zheng. 2009. Increased intratumoral IL-17-producing cells correlate with poor survival in hepatocellular carcinoma patients. *J. Hepatol.* 50:980–989. <http://dx.doi.org/10.1016/j.jhep.2008.12.033>
- Zheng, Y., P.A. Valdez, D.M. Danilenko, Y. Hu, S.M. Sa, Q. Gong, A.R. Abbas, Z. Modrusan, N. Ghilardi, F.J. de Sauvage, and W. Ouyang. 2008. Interleukin-22 mediates early host defense against attaching and effacing bacterial pathogens. *Nat. Med.* 14:282–289. <http://dx.doi.org/10.1038/nm1720>